ischemia up to 16 hours induced dysfunction of BC as characterized by their disappearance and dilation, while their polygonal networks were kept intact unless the duration of cold storage exceeded 8 hours. To our knowledge, it remains unknown whether or not such a nonnecrotic dysfunction of hepatocytes exposed to a relatively short period of cold ischemia could be mediated by postischemic responses of sinusoidal cells involving KCs. As this study shows, the reduced ability of hepatocytes to excrete organic anions via Mrp2 was completely restored by depleting KCs, suggesting involvement of these sinusoidal cells in the mechanisms of the dysfunction.

The impairment of Mrp2-mediated transport in the 8-hour post–cold ischemic grafts results from cytoplasmic relocalization of this transporter from canalicular membrane, not from disruption of BC networks or oxidative self-modification of the transporter. This is consistent with our previous observation that 8-hour cold ischemia and reperfusion does not exhibit evidence of oxidative stress in liver grafts.[14] Alterations in cAMP, a determinant for BC sorting of Mrp2,[32,40,41] are unlikely to play a role in the KC-mediated dysfunction, because its content did not differ irrespective of the presence of KCs. Hepatocellular content of ATP is another determinant of transporter function; however, it most likely plays a small role (if any) in the mechanisms, because any differences were not notable between the KC-depleting and control grafts having undergone 8-hour cold ischemia. Because KC depletion did not alter the ability of Mrp2 to excrete organic anions in normal livers, such an alteration of the transporter function in the grafts appears to result from responses of KCs that cannot be triggered unless the graft undergoes cold ischemia reperfusion. Although detailed mechanisms remain unknown, the present results suggest involvement of TXA_2 synthase, the enzyme responsible for TXs, a major class of prostanoids released from KCs.[37,38] The observation that the preventive effect of the enzyme inhibitor was completely cancelled in the KC-depleted grafts led us to suggest that KCs constitute a major source of TXs that trigger internalization of Mrp2 into the cytoplasm of hepatocytes. Although TXA_2 has been thought to exert potent biologic actions on various types of cells, previous studies provided evidence that TXB_2, a relatively stable metabolite of TXA_2, is able to activate nonlysosomal proteinases and thereby triggers bleb formation of primary cultured hepatocytes.[42] Thus, further mechanisms by which KC-derived TXs cause hepatocellular dysfunction should be necessary.

The newly developed method of dye exclusion analyses from grafts preloaded with controlled amounts of CF revealed that relocalization of Mrp2 occurs at hepatocellular levels and results in significant deterioration of the whole-graft function. As seen in Fig. 3, the 8-hour storage significantly reduced biliary glutathione excretion without showing any change in tissue content. Because this organic anion serves as the major substance yielding the osmotic driving force for bile acid–independent bile formation, its reduction in bile could result in a decrease in output. This notion is also consistent with our observation that 8-hour stored grafts displayed a significant reduction of output.

In this context, the imbalance between endogenous generation and biliary excretion of BR-IXα in the grafts is of great interest. As seen in Fig. 2, the control liver can excrete approximately 75% of endogenous BR-IXα into bile within 20 minutes of perfusion, which is consistent with our previous studies.[24] On the other hand, such a rapid elimination of bile pigment did not occur in the 16-hour cold ischemic grafts. As judged by biliary concentrations of BR-IXα (Fig. 2E), the absolute amounts of the pigment were elevated but never decreased compared with the non–cold ischemic control grafts. Because amounts of BR-IXα released into circulation were negligible (data not shown), these results suggest that the cold ischemic grafts synthesize greater amounts of the pigment during the initial 20-minute reperfusion than those expected from their capacity to excrete it into bile. This notion is in good agreement with our observation that the graft induces heme oxygenase-1, the stress-inducible enzyme for heme degradation.[43] This event is of pathophysiologic importance with regard to antioxidative stress responses of post–cold ischemic grafts. We have recently reported that low-dose bilirubin can ameliorate oxidative stress and thereby protect post–cold ischemic liver grafts, although it is obviously harmful in excessive doses.[31,43] In the grafts exposed to cold ischemia, reperfusion could cause two important events that critically dictate hepatic bilirubin metabolism: increased heme degradation and decreased excretion of BR-IXα through Mrp2. Thus, combined actions of these two events could result in accumulation of this antioxidant sufficient enough to protect hepatocytes, while their prolonged effects lead to hepatocellular damages and hyperbilirubinemia in the later period of reperfusion.

KCs are potent generators of eicosanoids, while hepatocytes and ATP-binding cassette transporters expressed on their membrane help their degradation and excretion, respectively.[38,39] On the other hand, antioxidant organic anions such as glutathione and bilirubin share Mrp for their excretion into bile in the post–cold ischemic grafts. Thus, the balance between KC-mediated synthesis of eicosanoids and their removal from hepatocytes could determine redistribution of the antioxidant anions in and around hepatocytes, thereby dictating functional out-

come of liver transplantation. KC-mediated remodeling of Mrp-mediated organic anion transport deserves further studies, provided that quantitative information on intra- and intercellular kinetics of glutathione and BR-IXα becomes available. Such studies could answer if KC-yielded TX could serve as an early alert mechanism against subsequent oxidative stress on liver grafts.

References

1. Ploeg RJ, D'Alessandro AM, Knechtle SJ, Stegall MD, Pirsch JD, Hoffmann RM, Sasaki T, et al. Risk factors for primary dysfunction after liver transplantation—a multivariate analysis. Transplantation 1993;55:807–813.
2. Deschenes M, Belle SH, Krom RA, Zetterman RK, Lake JR. Early allograft dysfunction after liver transplantation: a definition and predictors of outcome. National Institute of Diabetes and Digestive and Kidney Diseases Liver Transplantation Database. Transplantation 1998;66:302–310.
3. Porte RJ, Ploeg RJ, Hansen B, van Bockel JH, Thorogood J, Persijn GG, Hermans J, et al. Long-term graft survival after liver transplantation in the UW era: late effects of cold ischemia and primary dysfunction. European Multicentre Study Group. Transpl Int 1998;11(Suppl 1):S164–S167.
4. Adam R, Bismuth H, Diamond T, Ducot B, Morino M, Astarcioglu I, Johann M, et al. Effect of extended cold ischaemia with UW solution on graft function after liver transplantation. Lancet 1992;340:1373–1376.
5. Jaeschke H. Preservation injury: mechanisms, prevention and consequences. J Hepatol 1996;25:774–780.
6. Caldwell-Kenkel JC, Currin RT, Tanaka Y, Thurman RG, Lemasters JJ. Reperfusion injury to endothelial cells following cold ischemic storage of rat livers. HEPATOLOGY 1989;10:292–299.
7. Caldwell-Kenkel JC, Currin RT, Tanaka Y, Thurman RG, Lemasters JJ. Kupffer cell activation and endothelial cell damage after storage of rat livers: effects of reperfusion. HEPATOLOGY 1991;13:83–95.
8. Lemasters JJ, Thurman RG. Reperfusion injury after liver preservation for transplantation. Annu Rev Pharmacol Toxicol 1997;37:327–338.
9. Clavien PA. Sinusoidal endothelial cell injury during hepatic preservation and reperfusion. HEPATOLOGY 1998;28:281–285.
10. Sindram D, Porte RJ, Hoffman MR, Bentley RC, Clavien PA. Platelets induce sinusoidal endothelial cell apoptosis upon reperfusion of the cold ischemic rat liver. Gastroenterology 2000;118:183–191.
11. Arai M, Mochida S, Ohno A, Fujiwara K. Blood coagulation in the hepatic sinusoids as a contributing factor in liver injury following orthotopic liver transplantation in the rat. Transplantation 1996;62:1398–1401.
12. Clavien PA, Harvey PR, Sanabria JR, Cywes R, Levy GA, Strasberg SM. Lymphocyte adherence in the reperfused rat liver: mechanisms and effects. HEPATOLOGY 1993;17:131–142.
13. Vajdova K, Smrekova R, Mislanova C, Kukan M, Lutterova M. Cold-preservation-induced sensitivity of rat hepatocyte function to rewarming injury and its prevention by short-term reperfusion. HEPATOLOGY 2000; 32:289–296.
14. Kumamoto Y, Suematsu M, Shimazu M, Kato Y, Sano T, Makino N, Hirano KI, et al. Kupffer cell-independent acute hepatocellular oxidative stress and decreased bile formation in post-cold-ischemic rat liver. HEPATOLOGY 1999;30:1454–1463.
15. Imamura H, Brault A, Huet PM. Effects of extended cold preservation and transplantation on the rat liver microcirculation. HEPATOLOGY 1997;25: 664–671.
16. Williams JW, Vera S, Peters TG, Van Voorst S, Britt LG, Dean PJ, Haggitt R, et al. Cholestatic jaundice after hepatic transplantation. A nonimmunologically mediated event. Am J Surg 1986;151:65–70.
17. Suzuki H, Suematsu M, Ishii H, Kato S, Miki H, Mori M, Ishimura Y, et al. Prostaglandin E1 abrogates early reductive stress and zone-specific paradoxical oxidative injury in hypoperfused rat liver. J Clin Invest 1994;93: 155–164.
18. Suematsu M, Goda N, Sano T, Kashiwagi S, Egawa T, Shinoda Y, Ishimura Y. Carbon monoxide: an endogenous modulator of sinusoidal tone in the perfused rat liver. J Clin Invest 1995;96:2431–2437.
19. Kyokane T, Norimizu S, Taniai H, Yamaguchi T, Takeoka S, Tsuchida E, Naito M, et al. Carbon monoxide from heme catabolism protects against hepatobiliary dysfunction in endotoxin-treated rat liver. Gastroenterology 2001;120:1227–1240.
20. Goda N, Suzuki K, Naito M, Takeoka S, Tsuchida E, Ishimura Y, Tamatani T, et al. Distribution of heme oxygenase isoforms in rat liver. Topographic basis for carbon monoxide-mediated microvascular relaxation. J Clin Invest 1998;101:604–612.
21. Shiomi M, Wakabayashi Y, Sano T, Shinoda Y, Nimura Y, Ishimura Y, Suematsu M. Nitric oxide suppression reversibly attenuates mitochondrial dysfunction and cholestasis in endotoxemic rat liver. HEPATOLOGY 1998; 27:108–115.
22. Ishiguro S, Arii S, Monden K, Fujita S, Nakamura T, Niwano M, Harada T, et al. Involvement of thromboxane A_2-thromboxane A_2 receptor system of the hepatic sinusoid in pathogenesis of cold preservation/reperfusion injury in the rat liver graft. Transplantation 1995;59:957–961.
23. Jaeschke H, Smith CV, Mitchell JR. Reactive oxygen species during ischemia-reflow injury in isolated perfused rat liver. J Clin Invest 1988;81: 1240–1246.
24. Yamaguchi T, Wakabayashi Y, Tanaka M, Sano T, Ishikawa H, Nakajima H, Suematsu M, et al. Taurocholate induces directional excretion of bilirubin into bile in perfused rat liver. Am J Physiol 1996;270:G1028–G1032.
25. Izumi Y, Yamazaki M, Shimizu S, Shimizu K, Yamaguchi T, Nakajima H. Anti-bilirubin monoclonal antibody. II. Enzyme-linked immunosorbent assay for bilirubin fractions by combination of two monoclonal antibodies. Biochim Biophys Acta 1988;967:261–266.
26. Mor-Cohen R, Zivelin A, Rosenberg N, Shani M, Muallem S, Seligsohn U. Identification and functional analysis of two novel mutations in the multidrug resistance protein 2 gene in Israeli patients with Dubin-Johnson syndrome. J Biol Chem 2001;276:36923–36930.
27. van der Kolk DM, de Vries EG, Noordhoek L, van den Berg E, van der Pol MA, Muller M, Vellenga E. Activity and expression of the multidrug resistance proteins P-glycoprotein, MRP1, MRP2, MRP3 and MRP5 in de novo and relapsed acute myeloid leukemia. Leukemia 2001;15:1544–1553.
28. Courtois A, Payen L, Lagadic D, Guillouzo A, Fardel O. Evidence for a multidrug resistance-associated protein 1 (MRP1)-related transport system in cultured rat liver biliary epithelial cells. Life Sci 1999;64:763–774.
29. Suematsu M, Suzuki H, Ishii H, Kato S, Yanagisawa T, Asako H, Suzuki M, et al. Early midzonal oxidative stress preceding cell death in hypoperfused rat liver. Gastroenterology 1992;103:994–1001.
30. Kajimura M, Shimoyama M, Tsuyama S, Suzuki T, Kozaki S, Takenaka S, Tsubota K, et al. Visualization of gaseous monoxide reception by soluble guanylate cyclase in the rat retina. FASEB J 2003;17:506–508.
31. Hayashi S, Takamiya R, Yamaguchi T, Matsumoto K, Tojo SJ, Tamatani T, Kitajima M, et al. Induction of heme oxygenase-1 suppresses venular leukocyte adhesion elicited by oxidative stress: role of bilirubin generated by the enzyme. Circ Res 1999;85:663–671.
32. Mottino AD, Cao J, Veggi LM, Crocenzi F, Roma MG, Vore M. Altered localization and activity of canalicular Mrp2 in estradiol-17beta-D-glucuronide-induced cholestasis. HEPATOLOGY 2002;35:1409–1419.
33. Kubitz R, D'Urso D, Keppler D, Haussinger D. Osmodependent dynamic localization of the multidrug resistance protein 2 in the rat hepatocyte canalicular membrane. Gastroenterology 1997;113:1438–1442.
34. Uchida K, Kanematsu M, Sakai K, Matsuda T, Hattori N, Mizuno Y, Suzuki D, et al. Protein-bound acrolein: potential markers for oxidative stress. Proc Natl Acad Sci U S A 1998;95:4882–4887.
35. Tanaka N, Tajima S, Ishibashi A, Uchida K, Shigematsu T. Immunohistochemical detection of lipid peroxidation products, protein-bound acrolein and 4-hydroxynonenal protein adducts, in actinic elastosis of photodamaged skin. Arch Dermatol Res 2001;293:363–367.

36. Ogawa K, Suzuki H, Hirohashi T, Ishikawa T, Meier PJ, Hirose K, Akizawa T, et al. Characterization of inducible nature of MRP3 in rat liver. Am J Physiol Gastrointest Liver Physiol 2000;278:G438–G446.
37. Gyenes M, De Groot H. Prostanoid release by Kupffer cells upon hypoxia-reoxygenation: role of pHi and Ca^{2+}. Am J Physiol 1993;264:G535–G540.
38. Johnston DE, Peterson MB, Mion F, Berninger RW, Jefferson DM. Synthesis and degradation of eicosanoids in primary rat hepatocyte cultures. Prostaglandins Leukot Essent Fatty Acids 1991;43:119–132.
39. Nakamura J, Nishida T, Hayashi K, Kawada N, Ueshima S, Sugiyama Y, Ito T, et al. Kupffer cell-mediated down regulation of rat hepatic CMOAT/MRP2 gene expression. Biochem Biophys Res Commun 1999; 255:143–149.
40. Roelofsen H, Soroka CJ, Keppler D, Boyer JL. Cyclic AMP stimulates sorting of the canalicular organic anion transporter (Mrp2/cMoat) to the apical domain in hepatocyte couplets. J Cell Sci 1998;111:1137–1145.
41. Kipp H, Arias IM. Intracellular trafficking and regulation of canalicular ATP-binding cassette transporters. Semin Liver Dis 2000;20:339–351.
42. Horton AA,Wood JM. Prevention of thromboxane B2-induced hepatocyte plasma membrane bleb formation by certain prostaglandins and a proteinase inhibitor. Biochim Biophys Acta 1990;1022:319–324
43. Kato Y, Shimazu M, Kondo M, Uchida K, Kumamoto Y, Wakabayashi G, Kitajima M, et al. Bilirubin rinse: a simple protectant against the rat liver graft injury mimicking heme oxygenase-1 preconditioning. HEPATOLOGY 2003;38:364–373.

Role of Thromboxane Derived From COX-1 and -2 in Hepatic Microcirculatory Dysfunction During Endotoxemia in Mice

Hiroyuki Katagiri,[1] Yoshiya Ito,[1] Ken-ichiro Ishii,[1] Izumi Hayashi,[2] Makoto Suematsu,[4] Shohei Yamashina,[3] Takahiko Murata,[5] Shuh Narumiya,[5] Akira Kakita,[1] and Masataka Majima[2]

Although thromboxanes (TXs), whose synthesis is regulated by cyclooxygenase (COX), have been suggested to promote inflammation in the liver, little is known about the role of TXA_2 in leukocyte endothelial interaction during endotoxemia. The present study was conducted to investigate the role of TXA_2 as well as that of COX in lipopolysaccharide (LPS)-induced hepatic microcirculatory dysfunction in male C57Bl/6 mice. We observed during *in vivo* fluorescence microscopic study that LPS caused significant accumulation of leukocytes adhering to the hepatic microvessels and non-perfused sinusoids. Levels of serum alanine transaminase (ALT) and tumor necrosis factor alpha (TNFα) also increased. LPS raised the TXB_2 level in the perfusate from isolated perfused liver. A TXA_2 synthase inhibitor, OKY-046, and a TXA_2 receptor antagonist, S-1452, reduced LPS-induced hepatic microcirculatory dysfunction by inhibiting TNFα production. OKY-046 suppressed the expression of an intercellular adhesion molecule (ICAM)-1 in an LPS-treated liver. In thromboxane prostanoid receptor-knockout mice, hepatic responses to LPS were minimized in comparison with those in their wild-type counterparts. In addition, a selective COX-1 inhibitor, SC-560, a selective COX-2 inhibitor, NS-398, and indomethacin significantly attenuated hepatic responses to LPS including microcirculatory dysfunction and release of ALT and TNFα. The effects of the COX inhibitors on hepatic responses to LPS exhibited results similar to those obtained with TXA_2 synthase inhibitor, and TXA_2 receptor antagonist. In conclusion, these results suggest that TXA_2 is involved in LPS-induced hepatic microcirculatory dysfunction partly through the release of TNFα, and that TXA_2 derived from COX-1 and COX-2 could be responsible for the microcirculatory dysfunction during endotoxemia. (HEPATOLOGY 2004;39:139–150.)

The initial hepatic responses to lipopolysaccharide (LPS) include the activation of the nonparenchymal cells that constitute the hepatic microvascular system. The early events occurring in the hepatic microvasculature, including increases in leukocyte adhesion, reduction of sinusoidal perfusion, and activated Kupffer cells contribute to alterations in liver function caused by endotoxin.[1,2] However, the mechanisms by which LPS induces hepatic microcirculatory dysfunction are not fully understood.

Proinflammatory cytokines released from activated Kupffer cells including tumor necrosis factor alpha (TNFα)[3,4] are involved in the hepatic microvascular inflammatory response to LPS. Inactivation of Kupffer cells with gadolinium chloride ameliorates LPS-induced hepatic microcirculatory dysfunction, and this process was accompanied by a decrease in the plasma TNFα level.[2] The administration of TNFα causes a hepatic microcirculatory derangement similar to that produced by endotoxin.[5] In addition to cytokines, metabolites of arachidonic acid including prostaglandins (PGs) and thromboxanes (TXs) have been suggested to participate in liver injury during endotoxemia.[6] For example, a significant increase in the plasma level of TXB_2 (a stable metabolite of TXA_2) is shown after LPS administration.[7] The TXA_2 receptor antagonist exerts a protective effect on

Abbreviations: LPS, lipopolysaccharide; TNF, tumor necrosis factor; PG, prostaglandin; TX, thromboxane; COX, cyclooxygenase; TP, thromboxane-prostanoid; ALT, alanine aminotransferase; RT-PCR, reverse-transcription polymerase chain reaction; ICAM-1, intercellular adhesion molecule-1; PECAM-1, platelet-endothelial cell adhesion molecule-1; mRNA, messenger RNA.

From the Departments of [1]Surgery, [2]Pharmacology, and [3]Anatomy, Kitasato University School of Medicine, Kanagawa, Japan; the [4]Department of Biochemistry and Integrative Medical Biology, Keio University, Tokyo, Japan; and the [5]Department of Pharmacology, Kyoto University, Kyoto, Japan.

Received January 17, 2003; accepted October 22, 2003.

Supported by grants from an Integrative Research Program of the Graduate School of Medical Science, Kitasato University, and from Parents' Association Grant of Kitasato University School of Medicine. This work was also supported by a research grant (#15390084), by a "High-tech Research Center" grant, and by a grant from The 21st Century COE Program, from Ministry of Education, Culture, Sports, Science and Technology (MEXT).

Address reprint requests to: Masataka Majima, Kitasato University School of Medicine, 1-15-1 Kitasato, Sagamihara, Kanagawa 228-8555, Japan. E-mail: en3m-mjm@asahi-net.or.jp; fax: +81-42-778-9556.

Published online in Wiley InterScience (www.interscience.wiley.com).

DOI 10.1002/hep.20000

liver injury caused by endotoxin.[8] Furthermore, PGs and TXs modulate TNFα synthesis. PGE_2 suppresses TNFα production from Kupffer cells stimulated with endotoxin,[9] while TXA_2 synthase inhibitor suppresses TNFα release from peritoneal macrophages.[7] These results suggest that TXA_2 could augment leukocyte-endothelial interaction during endotoxemia by affecting the production of TNFα.

The synthesis of TXA_2 is regulated by cyclooxygenase (COX), which catalyzes the conversion of arachidonic acid to PGs and TXs. Two isoforms of the enzyme have been identified. The isoform designated COX-1 is constitutively expressed in most tissues, while the isoform designated COX-2 is inducible by a variety of factors, such as cytokines and endotoxin.[10] Indeed, the expression of COX-2 protein was induced in LPS-treated liver from rats.[11] The liver injury caused by LPS sensitized with galactosamine was minimized in COX-2 deficient mice.[12] Inhibition of COX-2 protects the liver[13] against injury from ischemia/reperfusion. These results indicate that COX-2 contributes to liver injury. However, much remains unknown about the involvement of 2 isoforms of COX (COX-1 and COX-2) in hepatic microcirculatory dysfunction during endotoxemia.

The present study was thus conducted to examine the effects of the inhibition of TXA_2 synthase and of the blockade of TXA_2 receptor on the hepatic microvascular response to LPS in mice using *in vivo* microscopic methods. Some of the experiments were performed with thromboxane prostanoid (TP)-receptor knockout mice to elucidate the role of endogenously produced TXA_2 in this response. We also investigated the effects of selective inhibition of COX-1 and COX-2 on LPS-induced hepatic microcirculatory dysfunction.

Materials and Methods

Drugs. Endotoxin (LPS from *Escherichia coli*, serotype 055:B5) was purchased from List Biological Laboratories (Campbell, CA). The selective TXA_2 synthase inhibitor OKY-046 ((E)-3-[p-(1H-imidazolmethyl)-phenyl]-2-propenoic acid) was supplied from Kissei Pharmaceutical (Osaka, Japan). The TXA_2 receptor antagonist S-1452 (14) (calcium (1R, 2S, 3S, 4S)-(5Z)-7(((phenylsulphonyl)-amino)-bicyclo-(2.2.1)-hept-2-yl) hept-5-heptenoate dihydrate) was supplied by Shionogi Pharmaceutical (Osaka, Japan). The selective COX-1 inhibitor SC-560 (15) (5-(4-chlorophenyl)-1-(4-methoxyphenyl)-3-trifluoromethylpyrazole) was obtained from Searle (St. Louis, MO). The selective COX-2 inhibitor NS-398 (16) (N-[2-(cyclohexyloxy)-4-nitrophenyl]-methanesulfonamide) was obtained from Cayman Chemical (Ann Arbor, MI). The nonselective COX inhibitor indomethacin was purchased from Merck (Rahway, NJ). The NS-398, SC-560, indomethacin, and S-1452 were suspended in 5% gum arabic, while the OKY-046 was dissolved in physiological saline. Anti-mouse lymphocyte function associated antigen (LFA)-1 monoclonal antibody was purchased from Endogen (Woburn, MA).

Animals. Male C57BL/6 mice (6–8 weeks of age), weighing 20–25g, were obtained from Shizuoka Laboratory Animal Center (Hamamatsu, Japan). TP receptor-knockout mice ($TP^{-/-}$, male, 8 weeks of age) were developed by us.[17] A genetic background of TP-receptor knockout mice is similar to that of C57BL/6 mice. They were maintained at a constant humidity (60 ± 5%) and temperature (25 ± 1 °C) and were kept continuously on a 12-hour light/dark cycle. All animals were provided food and water *ad libitum*. All procedures on animals were performed in accordance with the guidelines for animal experiments of Kitasato University School of Medicine.

Experimental Protocols for* In Vivo *Microscopic Study. LPS was injected intravenously (0.3 mg/kg in 0.1 ml of physiological saline) into mice through the tail vein. OKY-046 (50 mg/kg in 0.1 ml saline, intravenously), S-1452 (10 mg/kg, per os), SC-560 (10 mg/kg, per os), NS-398 (10 mg/kg, subcutaneous injection), indomethacin (10 mg/kg, per os), and vehicle (10 mg/kg, per os) were administered 30 min before LPS injection. Some animals were treated with 2 mg/kg (intravenously) of the LFA-1 monoclonal antibody simultaneously with LPS injection. The dose regimens of the specific inhibitors, including NS-398 and SC-560, used in the present study were based on their inhibitory effects on activity against COX-1 or COX-2.[15,16]

Preparation for* In Vivo *Microscopy. Four hours after LPS injection, animals anesthetized with pentobarbital sodium (50 mg/kg, intraperitoneally) were prepared for *in vivo* fluorescence microscopy according to modifications of methods previously described.[5] After transverse laparotomy, the animals were positioned on their left side and placed on a stage. The left lobe of the liver was pulled gently and covered with a thin cover glass to stabilize its position and limit movement induced by respiration. The hepatic microcirculation was observed at the surface of the liver using a fluorescence microscope (X2-UD, upright type; Nikon, Tokyo) with a 100-W mercury lamp for epi-illumination. The microscopic images were obtained with a long working distance objective lens (M plan 20/0.20 SLWD; Nikon, Tokyo) and a ×5 eyepiece lens. Images of the hepatic microcirculation were transmitted through a silicon-intensified target camera (C2400-08; Hamamatsu Photonics; Hamamatsu) to a TV monitor screen (PVM-1444Q; Sony, Tokyo) and

were recorded on videotape with an S-VHS recorder (BR-S600; Victor, Tokyo).

For contrast enhancement of the plasma, FITC-labeled dextran (Sigma, St. Louis, MO) was intravenously administered (4 mg/kg) just before the start of the observation. Leukocytes were labeled with 0.3 μmol/kg of rhodamine-6G (Sigma) at the same time.[18] FITC-dextran and rhodamine-6G were visualized by epi-illumination with filter combination of 420 to 490 nm/ > 520 nm (excitation/emission) and 510 to 560 nm/ > 590 nm, respectively.

Analysis of* In Vivo *Microscopy. To examine the interaction of leukocytes with endothelium, the number of leukocytes adhering was determined off-line during video playback analysis. A leukocyte was defined as adhering to the venular and sinusoidal walls if it remained stationary for more than 20 seconds. With respect to the leukocytes adhering to the venules, 5 to 8 portal or central venules per animal were observed and assessed. The endothelial surface area of each venule was measured from video recordings using an adjustable electric microscaler (Argus-10; Hamamatsu Photonics; Hamamatsu). We determined the adherence of leukocytes in terms of 1) numbers of adhering leukocytes in the sinusoids per microscopic field (X100), and 2) numbers of adhering leukocytes in the portal and central venules per 1000 μm^2 of endothelial surface.

The sinusoidal perfusion deficits were evaluated by counting the number of non-perfused sinusoids in the same microscopic field as that in which the number of adhering leukocytes was determined. The percentage of non-perfused sinusoids was calculated as the ratio of the number of non-perfused sinusoids to the total number of all visible sinusoids. The results were expressed as the percentage of non-perfused sinusoids.

Sampling and Assays. In a separate set of experimental animals, blood was collected from the heart. The serum activity of alanine aminotransferase (ALT) was measured by an automated procedure with an analyzer. The plasma concentration of TNFα was measured with an enzyme-linked immunoabsorbent assay kit (Biosource International Inc, Camarillo, CA).

Experimental Procedure for Perfusion of the Isolated Liver. The isolated non-recirculating perfused liver system was prepared according to the method of Suematsu et al.[19] with some minor modification. In brief, mice were anesthetized with pentobarbital sodium (50 mg/kg, intraperitoneally) and were heparinized (100 units/mouse) to avoid blood coagulation in the liver. After transverse laparotomy, the portal vein was cannulated with a 24-gauge catheter. Immediately after the cannulation, the liver was initially perfused with a sterile, hemoglobin- and albumin-free Krebs-Henseleit bicarbonate buffered solution (pH 7.4, 37 °C) gassed with carbogen (95% O_2, 5% CO_2). After the start of perfusion of the liver, the inferior vena cava was cut, and the liver was removed. The perfusate was pumped through the isolated liver at a constant flow rate (4.0 ml/min) while the portal perfusion pressure was monitored and maintained at a level of 2 to 4 cmH_2O. Before collection of the first sample, the isolated liver was perfused for 20 min to eliminate blood elements and to stabilize it. Samples of the hepatic effluent emerging from the inferior vena cava were collected every 5 min to determine the amount of TXB_2. The levels of TXB_2 were measured with separate enzyme-linked immunoabsorbent assays (Cayman Chemical) as described previously.[20,21]

Experimental Protocols for Perfusion Experiment. Four experimental groups of animal livers were set up to investigate whether the liver is a site of TXA_2 production. In the 1st group, the livers of wild-type mice perfused with buffer solution throughout the experiment served as controls. In the 2nd and 3rd groups, 30 min after the start of perfusion, the administration of LPS (1.25 μg/min for 20 min) was initiated to TP-receptor knockout mice and to their wild-type counterparts and was continued throughout the experimental period. In the 4th group, 30 min before the start of preparation for the perfusion experiment, wild-type mice were treated with OKY-046 (50 mg/kg, intravenously), and OKY-046 (0.05 μg/min for 50 min) was administered simultaneously with the start of the perfusion with buffer. At 30 min after the start of perfusion, LPS (1.25 μg/min for 20 min) was continuously infused until the end of the experimental period.

Reverse-Transcription Polymerase Chain Reaction Analysis. Four hours after LPS injection, approximately 100 mg of the liver tissue was excised and was homogenized in 1 ml of Trizol Reagent (GIBCO BRL, Rockville, MD) with Polytrone (Kinematica GmbH, Luzern, Switzerland). A sample of RNA was extracted from the tissue in accordance with the manufacturer's instructions. Single-stranded complementary DNA was synthesized from 250 ng of total RNA using 0.4 μg of oligo-p(dT)15 primer and 4 units of AMV reverse transcriptase (Roche Diagnostics, Basel, Switzerland). PCR was performed in 10 μl of 20 mM Tris-HCl (pH 8.7) and 0.5 unit of Taq DNA polymerase (Qiagen GmbH, Germany). The oligonucleotide primers used were for reverse-transcription polymerase chain reaction (RT-PCR) analysis as follows: for mouse COX-1, 5′-TTGCACAACACTTCACCCACCAG–3′ (sense), 5′-AAACACCTCCTGGCCCACAGCCAT–3′ (antisense) (276 bp); mouse COX-2, 5′-GGAGAGAAGGAAATGGCTGCA–3′ (sense), 5′-ATCTAGTCTGGAGTGGGAGG–3′ (antisense) (363

bp); intercellular adhesion molecule (ICAM)-1, 5′-CGGGATCCAGGAAAGCCAAGGCCAAA-3′ (sense) and5′-CGGAATTCTTGACTGTCTTAA-GTTCC-3′ (antisense) (326 bp); platelet-endothelial cell adhesion molecule (PECAM)-1, 5′-CGGGATCCAG-GAAAGCCAAGGCCAAA-3′ (sense) and 5′-CG-GAATTCTTGACTGTCTTAAGTTCC-3′ (antisense) (348 bp); glyceraldehyde-3-phosphate dehydrogenase (GAPDH), 5′-CCCTTATTGACCTCAACTACAT-GGT-3′ (sense) and 5′-GAGGGGCCATCCACA-GTCTTCTG-3′ (antisense) (470 bp). These PCRs were run for 40 cycles. Cycling conditions were: 94 °C, 30 sec; 54 °C, 45 sec; and 72 °C, 45 sec for COX-1, ICAM-1, PECAM-1 and GAPDH, followed by a final extension for 10 min at 72 °C. For the amplification of COX-2, annealing was performed at 50 °C for 45 sec. Products of PCR were analyzed using 1.8% agarose gel electrophoresis, and the size of products was predicted from the sequences.

Immunohistochemical Studies. Immunohistochemical studies were performed as described elsewhere[22]. The sections from the paraffin-embedded tissues were incubated with rabbit anti-murine COX-1 or COX-2 antiserum (1:200 dilution, Cayman), or with rat anti-murine ICAM-1 antibody (1:100 dilution, 1A29, Biotechnology, Oxford) or rat anti-murine PECAM-1 antibody (1:100 dilution, MEC 13.3, PharMingen) at 4 °C overnight. These immunoreactivities were visualized using avidin-biotin-peroxydase complex (Vectastain ABC Kit, Vector Lab., Burlingame, CA).

Statistical Analysis. All data were expressed as means ± SEM. Multiple comparisons were carried out using 1-way ANOVA followed by Fisher's test. Differences were considered to be significant for P values less than .05.

Results

Figure 1 shows the *in vivo* fluorescence micrographs of hepatic microvasculature 4 hours after LPS injection. Leukocytes were seen adhering to the sinusoids as well as to the central venules (Fig. 1A). The sinusoidal perfusion deficits were also observed (Fig. 1B). In an additional group of experiments, we observed that the mean systemic arterial blood pressure 4 hours after LPS injection (109.3 ± 5.4 mmHg) did not change significantly when compared with that before LPS treatment (107.5 ± 5.6 mmHg) (n = 4).

The administration of LPS caused significant increases in the numbers of leukocytes adhering to the portal venules (8.5-fold) (Fig. 2A), sinusoids (50.2-fold) (Fig. 2B), and central venules (51.0-fold) (Fig. 2C) in comparison with those in saline-treated mice. Pre-treatment with OKY-046 lowered those by 61%, 46%, and 45.0%, respectively. Pre-treatment with S-1452 also suppressed those by 69%, 48%, and 39.0%, respectively. Concomitantly, the percentage of non-perfused sinusoids after LPS injection was increased (7.1-fold) (Fig. 2D). The percentage of non-perfused sinusoids was significantly lowered by OKY-046 (by 61.0%) and S-1452 (by 47.0%), respectively.

OKY-046 decreased the levels of plasma ALT activity at 4 hours after and the levels of plasma TNFα at 1 hour after LPS injection by 22% and 31%, respectively.

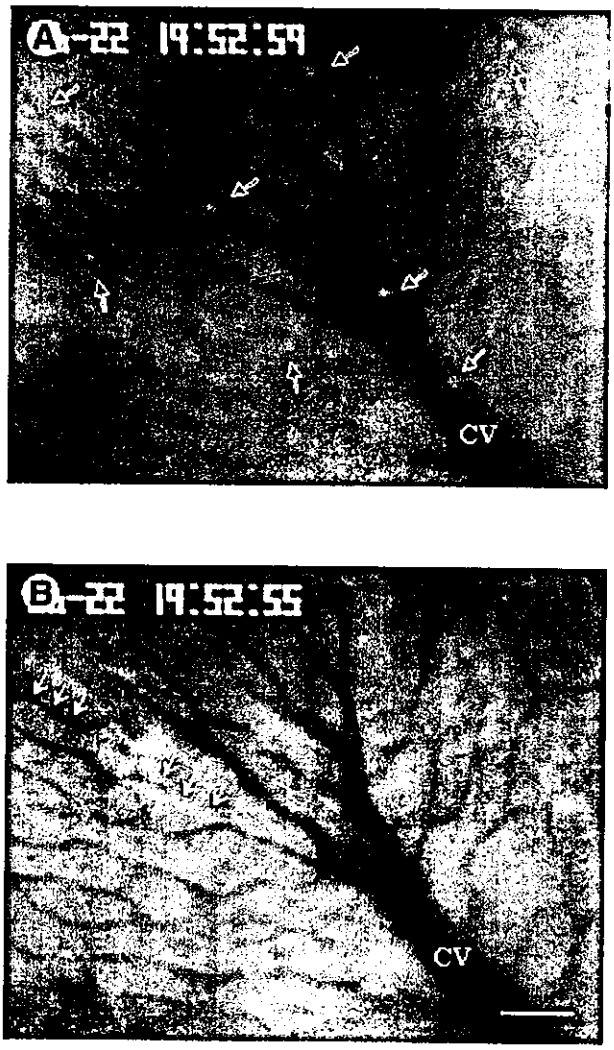

Fig. 1. Representative *in vivo* fluorescence micrographs of the hepatic microcirculation 4 hours after LPS injection. (A) Numerous leukocytes (**open arrows**), which were labeled with rhodamine 6G, adhere to the sinusoids and to the central venules. (B) The sinusoids and hepatic venules were well visualized by the injection of FITC-dextran. The sinusoidal perfusion deficits were detected by direct observation of the microcirculation as evidenced by the cessation of the perfusion (**arrows**) and by the non-visualization of the sinusoids (**arrowheads**). The fluorograph in Fig. 1B shows the same microscopic field as that in Fig. 1A. Bar represents 50 μm.

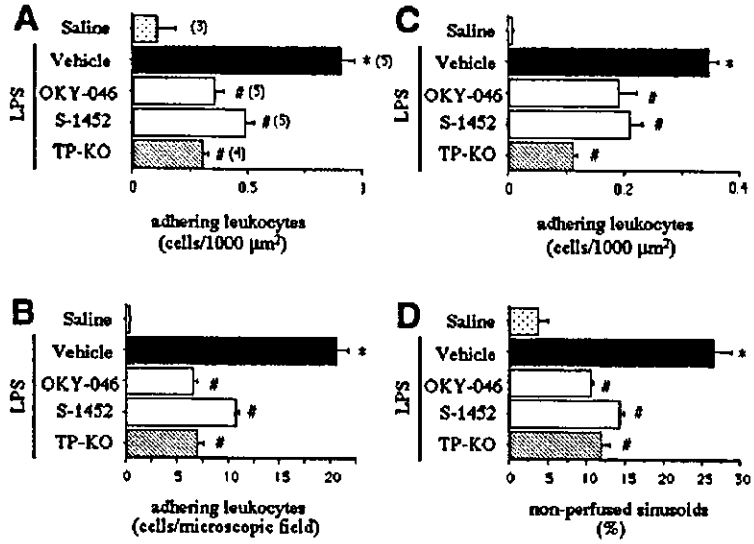

Fig. 2. Effects of LPS on (A) the numbers of leukocytes adhering to the portal venules, (B) the numbers of leukocytes adhering to the sinusoids, (C) the numbers of leukocytes adhering to the central venules, and (D) the percentage of non-perfused sinusoids, all in TP receptor-knockout (KO) mice and in their wild-type counterparts treated with OKY-046 (50 mg/kg, intravenously) and S-1452 (10 mg/kg, p.o.). Numbers in parentheses indicate number of animals. Data are shown as means ± SEM. *$P < .05$ versus Saline-treated mice; #$P < .05$ versus LPS-treated mice.

S-1452 also reduced them by 17% and 40%, respectively (Fig. 3).

To further investigate whether LPS-induced hepatic microcirculatory dysfunction is mediated by endogenously produced TXs, we used TP receptor-knockout mice. As shown in Fig. 2, in wild-type counterparts, LPS caused significant hepatic microcirculatory dysfunction as described above (Figs. 2A–D). In TP receptor-knockout mice, the numbers of leukocytes adhering to the portal venules, sinusoids, and central venules were significantly lower than in wild-type counterparts. Also the percentage of non-perfused sinusoids was lower in TP receptor-knockout mice than in wild-type mice. The levels of ALT and TNFα after LPS administration in TP receptor-knockout mice were decreased by 18% and 28%, respectively (Fig. 3).

Figure 4 illustrates changes in the levels of TXB_2 in the effluent perfusate from isolated perfused liver. The perfusion experiments were performed to determine whether there was a release site of TXA_2 by liver cells. In controls, no significant change in TXB_2 levels appeared (Fig. 4A). Within 15 min of the start of LPS administration, TXB_2 levels were rapidly increased in comparison with the baseline, and then continued to increase (Fig. 4B). Treatment of wild-type mice with OKY-046 completely abolished the increment of TXB_2 in response to LPS (Fig. 4C). In TP receptor-knockout mice, changes in TXB_2 levels after LPS were similar to those in the wild-type counterparts (Fig. 4D). During the perfusion experiment, the perfusion pressure was stable (2~4 cmH_2O) at all time points.

To investigate whether attenuation of hepatic microcirculatory dysfunction by TXA_2 inhibition affected the expression of adhesion molecules, the expression of ICAM-1 and PECAM-1 in the liver was assessed by RT-PCR and by immunohistochemistry (Figs. 5 and 7). LPS resulted in enhanced hepatic expression of messenger RNA (mRNA) of ICAM-1 when compared with that in saline-treated mice (Fig. 5A). OKY-046 partially prevented LPS-induce increase in ICAM-1 mRNA expression. The reduction in ICAM-1 mRNA expression was also seen in TP receptor-knockout mice.

The immunoreactivity with ICAM-1 was demonstrated in the sinusoids of saline-treated mice (Fig. 5B). LPS upregulated ICAM-1 expression in the sinusoids, as well as the hepatic venules (Fig. 5C), and OKY-046 reduced the ICAM-1 immunoreactivity (Fig. 5D).

To examine the significant contribution of ICAM-1 to leukocyte adhesion to the hepatic microvessels, mice were treated with monoclonal antibody against LFA-1, which is a ligand of ICAM-1. As shown in Fig. 6, the anti-LFA-1

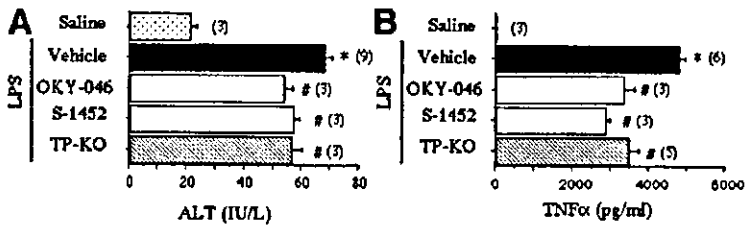

Fig. 3. Effects of LPS on (A) serum ALT activity and (B) the serum concentrations of TNFα in TP receptor-knockout (KO) mice and in their wild-type counterparts treated with OKY-046 (50 mg/kg, intravenously) and S-1452 (10 mg/kg, p.o.). Numbers in parentheses indicate number of animals. Data are shown as means ± SEM. *$P < .05$ versus Saline-treated mice; # $P < .05$ versus LPS-treated mice.

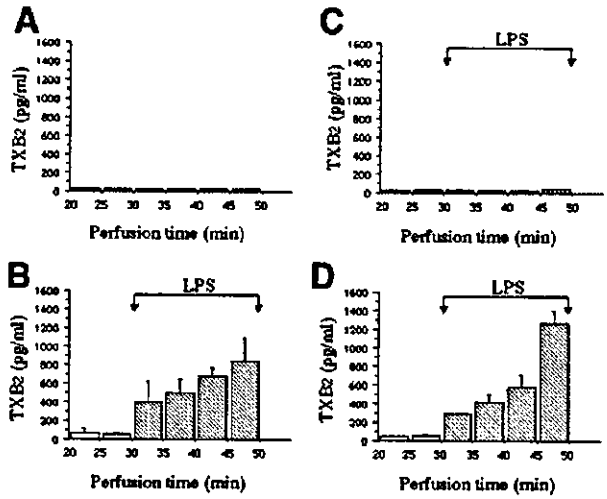

Fig. 4. Changes in the levels of TXB_2 in the effluent perfusate from the isolated perfused livers of wild-type mice (A,B,C) and of TP receptor-knockout mice (D). Livers from LPS-treated wild-type mice (B) and of TP receptor-knockout mice (D). Livers perfused with KH buffer solution alone throughout the experiment served as controls (A). Livers from wild-type mice treated with a combination of OKY-046 (0.05 μg/min for 50 min) and LPS (1.25 μg/min for 20 min) (C). Data are shown as means ± SEM from 3 animals.

antibody minimized hepatic microcirculatory dysfunction in response to LPS.

LPS resulted in slightly enhanced hepatic expression of mRNA of PECAM-1 when compared with that in saline-treated mice, and OKY-046 slightly reduced the expression of PECAM-1 in response to LPS (Fig. 7A). In results of immunohistochemical study, PECAM-1 was demonstrated in saline-treated mice liver (Fig. 7B). LPS enhanced expression of PECAM-1 weakly in comparison with that of ICAM-1 (Fig. 7C). OKY-046 did not affect PECAM-1 expression induced by LPS (Fig. 7D).

Because our results indicate that the hepatic microcirculatory dysfunction is mediated by TXA_2, and because TXA_2 is regulated by COX, we detected the expression of mRNA for COXs using RT-PCR. As shown in Fig. 8, in wild-type counterparts, COX-1 mRNA was expressed in both saline- and LPS-treated livers, whereas the expression of COX-2 mRNA was observed in an LPS-treated liver, but not in a saline-treated liver. The same was true for the livers of TP receptor-knockout mice.

The immunoreactivity with COX-1 in the saline-treated liver (Fig. 9A) and LPS-treated liver (Fig. 9B) was

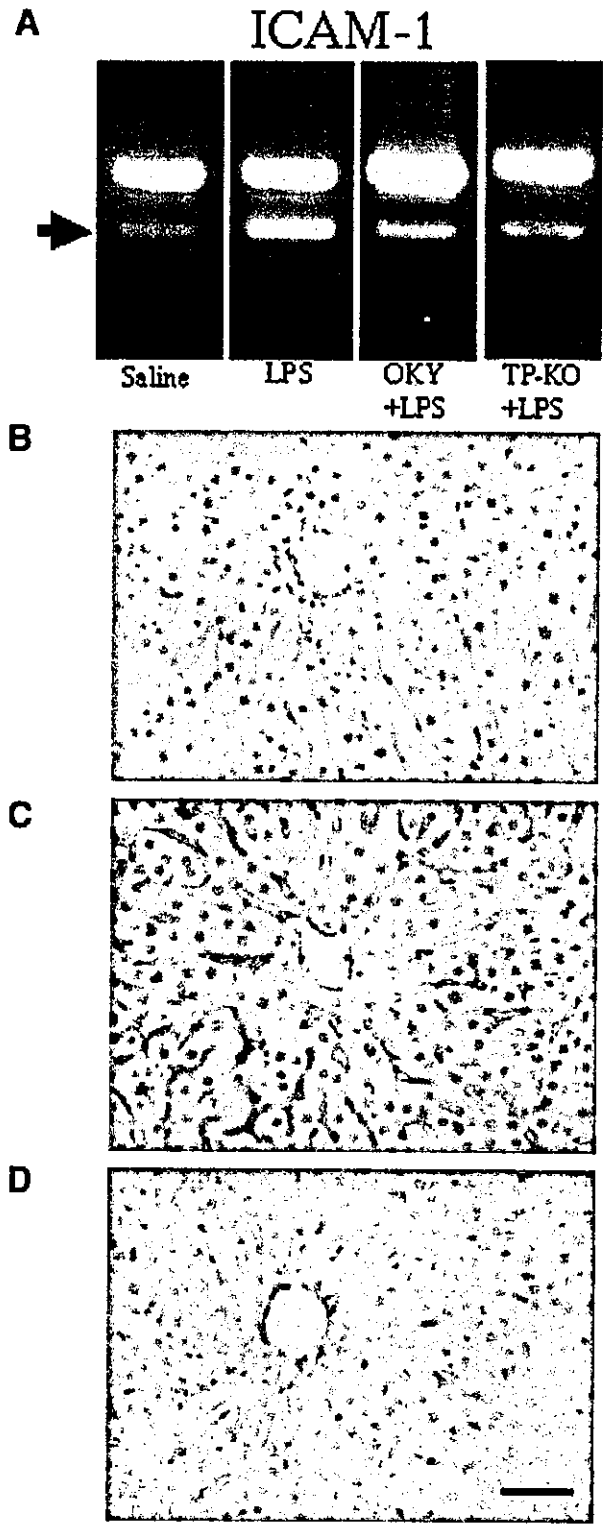

Fig. 5. Hepatic expression of ICAM-1 by RT-PCR analysis (A) and by immunohistochemical staining (B,C,D) 4 hours after LPS administration. LPS enhanced the expression of ICAM-1 mRNA in the liver (A). The hepatic expression of ICAM-1 mRNA after LPS was reduced in mice treated with OKY-046 and in TP- receptor-knockout mice. Immunoreactive ICAM-1 was seen in the sinusoidal lining cells in saline-treated mice (B). LPS enhanced ICAM-1 expression (C), and OKY-046 reduced the expression of ICAM-1 in LPS-treated liver (D). One representative experiment of 2 animals was presented. Bar indicates 50 μm.

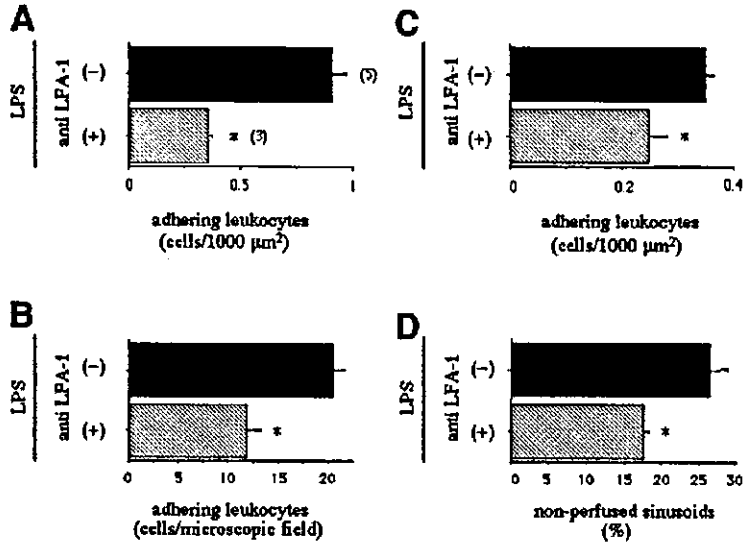

Fig. 6. Effects of an anti-LFA-1 antibody on (A) the numbers of leukocytes adhering to the portal venules, (B) the numbers of leukocytes adhering to the sinusoids, (C) the numbers of leukocytes adhering to the central venules, and (D) the percentage of non-perfused sinusoids at 4 hours after LPS administration. Numbers in parentheses indicate number of animals. Data are shown as means ± SEM. $*P < .05$ versus LPS-treated mice.

detected on the surface of hepatic microvessels. In contrast, the staining of COX-2 was negative in the saline-treated liver (Fig. 9C), however, the immunoreactive COX-2 in the LPS-treated liver was observed on the surface of the sinusoidal lining cells and on the hepatic venules. The most intense staining was shown in the sinusoids (Fig. 9D).

To ascertain which COX isozymes contribute to LPS–induced hepatic microcirculatory dysfunction, mice were pre-treated with SC-560, NS-398, and indomethacin. SC-560, NS-398, and indomethacin significantly lowered the numbers of leukocytes adhering to the portal venules (Fig. 10A), sinusoids (Fig. 10B), and central venules (Fig. 10C), respectively. In sinusoids, indomethacin lowered the numbers of adhered leukocytes more than SC-560 or NS-398 (Fig. 10B). The percentages of non-perfused sinusoids after LPS administration also were lower in mice treated with SC-560, NS-398, or indomethacin than in mice treated with vehicle (Fig. 10D). SC-560, NS-398, and indomethacin themselves did not significantly change leukocyte adhesion and sinusoidal perfusion in saline-treated mice (data not shown).

Four hours after LPS injection, the levels of ALT were significantly increased (3.2-fold) in comparison with the saline-treated controls (Fig. 11A). SC-560, NS-398, and indomethacin significantly decreased ALT levels after LPS injection by 35.0%, 42.0%, and 42.0%, respectively. The levels of TNFα 1 hour after LPS injection were significantly increased (Fig. 11B). SC-560, NS-398, and indomethacin significantly decreased TNFα levels, by 49.0%, 30.0%, and 33.0%, respectively.

Discussion

The results of the present study showed that OKY-046, a TXA_2 synthase inhibitor and S-1452, a TXA_2 receptor antagonist attenuated LPS-induced hepatic microcirculatory dysfunction as indicated by an increase of leukocytes adhering to the hepatic microvessels, as well as by impaired sinusoidal perfusion. To rule out the possibility that LPS affects the systemic hemodynamics, we measured the arterial blood pressure. The administration of LPS at a dose of 0.3 mg/kg (intravenously) did not reduce the mean arterial blood pressure. The hepatic microcirculatory dysfunction in response to LPS was accompanied by decreases in the serum levels of ALT and TNFα. These results suggest that TXA_2 enhances hepatic microcirculatory dysfunction during endotoxemia. This possibility was supported by our finding that TP receptor-knockout mice minimized liver injury and hepatic microcirculatory dysfunction in response to LPS by inhibiting TNFα production.

The finding that TXA_2 appears to modulate TNFα production after LPS administration (Fig. 3) is consistent with the findings of others,[7,27,28] that TXA_2 synthase inhibitor and TXA_2 receptor antagonist suppress LPS-induced TNFα release from macrophages[7,27] and from the perfused heart.[28] The inhibitory effects of OKY-046 and S-1452 on TNFα production in response to LPS were partial (30–40% reduction), while OKY-046 completely inhibited TXB_2 release in perfusate from the LPS-treated liver. These results suggest that other factors may be involved in the regulation of TNFα generation.

We observed that OKY-046 prevented the LPS-induced increase in ICAM-1 expression in the intrahepatic

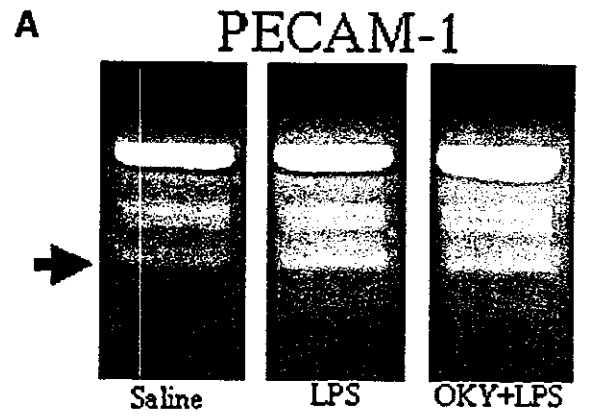

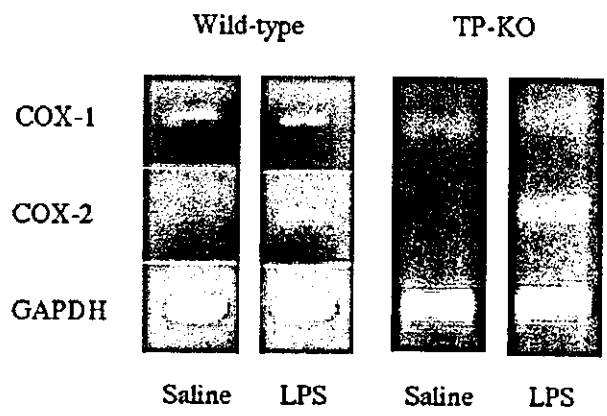

Fig. 8. Expression of COXs in liver tissue by RT-PCR analysis. Liver tissue was excised 4 hours after saline or LPS administration in wild-type and TP receptor-knockout (KO) mice. One representative experiment of 2 animals were presented.

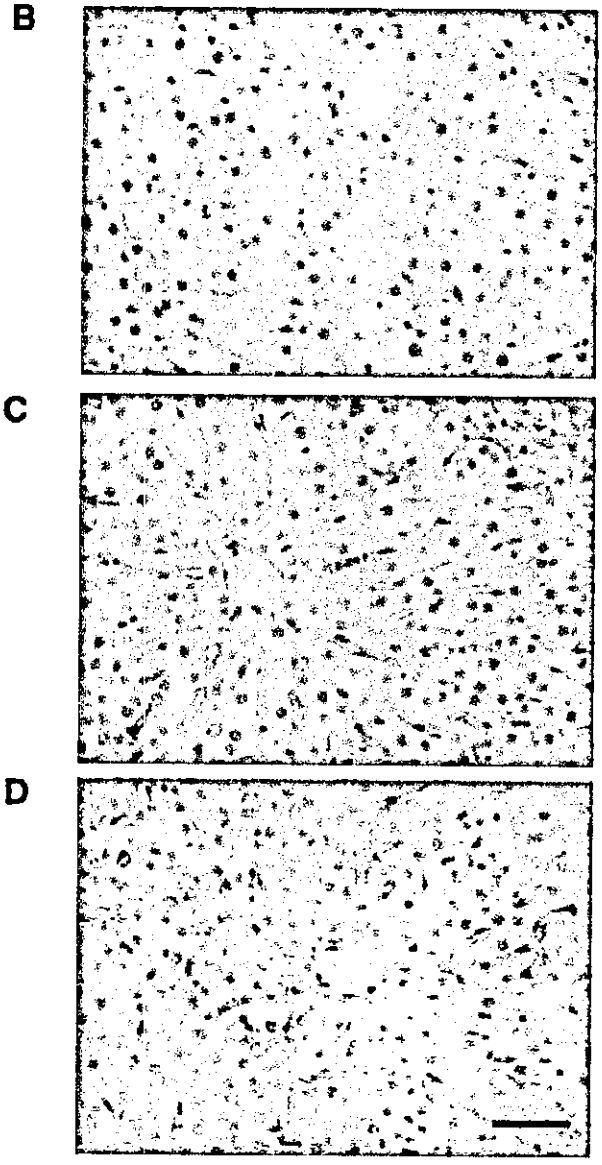

circulation, and that TP-receptor knockout mice exhibited decreased expression of ICAM-1 in the LPS-treated liver (Fig. 5). It has been reported that TXA_2 receptor antagonist suppresses the expression of ICAM-1 on human umbilical vein endothelial cells.[29] These findings suggest that increased ICAM-1 expression mediated by TP-receptor signaling may have facilitated leukocyte adhesion in the liver during endotoxemia. However, it is well known that TNFα released from Kupffer cells in response to LPS induces the transcriptional activation of ICAM-1 expression on the hepatic microvessels independently through TXA_2 signaling,[30] and that TNFα is the central mediator responsible for upregulation of hepatic ICAM-1 expression in response to hepatotoxicants such as carbon tetrachloride[31] and endotoxin.[32]

Enhanced ICAM-1 expression in the liver has been shown to contribute to leukocyte adhesion to the hepatic venules as well as to the sinusoids.[30] Our findings that the anti-LFA-1 antibody attenuated leukocyte adhesion indicates that ICAM-1 is involved in leukocyte adhesion in the endotoxemic liver. These results also suggest that attenuation of hepatic microcirculatory dysfunction is attributable to the reduction of ICAM-1 expression by

Fig. 7. Expression and immunoreactivity of PECAM-1 in liver tissue by RT-PCR analysis (A) and immunohistochemical staining (B,C,D) in liver tissue from mice treated with saline, LPS, and OKY-046/LPS. LPS resulted in slightly enhanced hepatic expression of mRNA of PECAM-1 when compared with that in saline-treated mice, and OKY-046 slightly reduced the expression of PECAM-1 in response to LPS (Fig. 7A). The immunoreactivity with PECAM-1 in saline-treated liver was weak (B), and was slightly enhanced in LPS-treated liver (C). OKY-046 did not change significantly the expression of PECAM-1 in LPS-treated liver (D). Liver tissue was excised 4 hours after LPS administration. One representative experiment of 2 animals was presented. Bar indicates 50 μm.

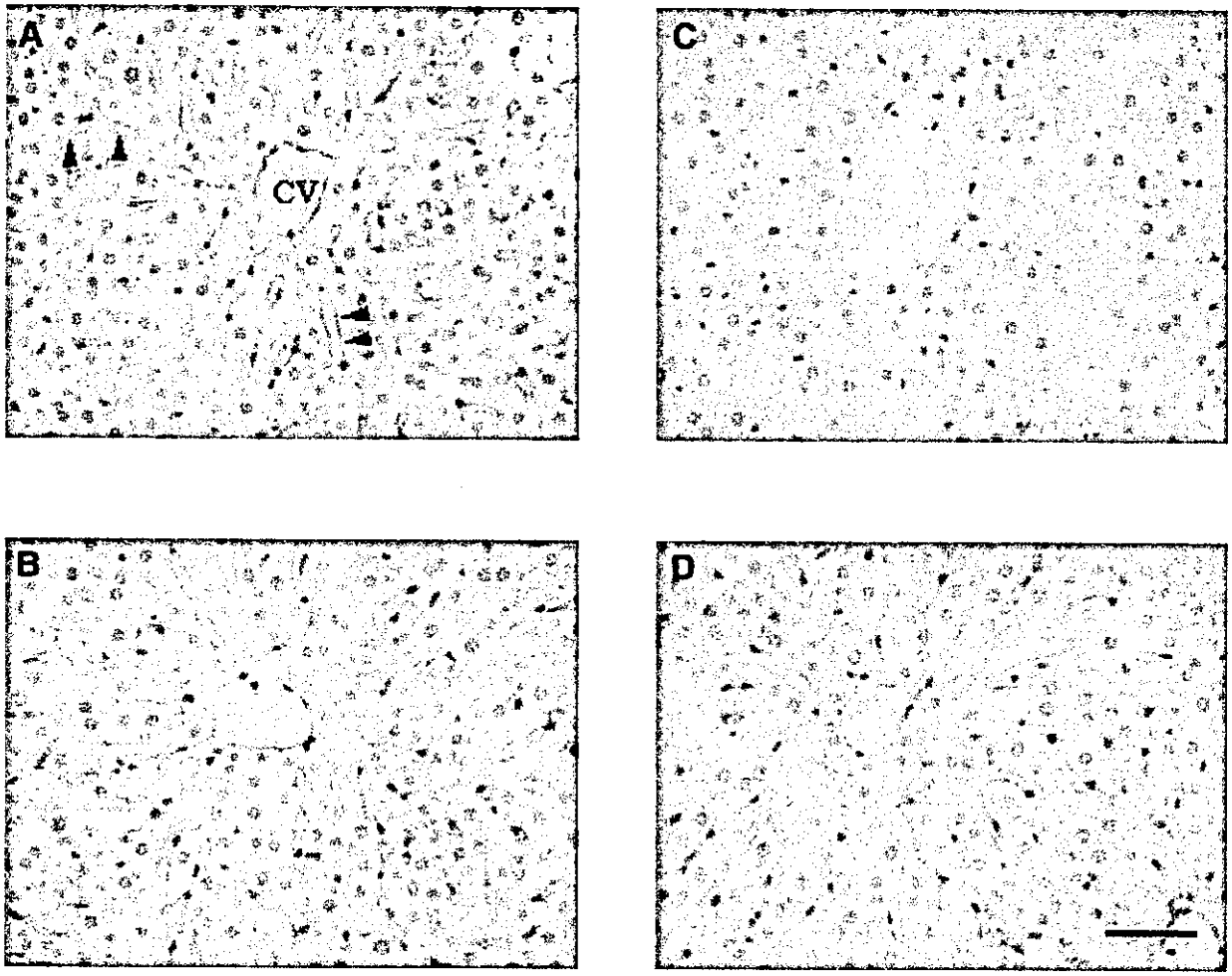

Fig. 9. Immunohistochemical localization of COX-1 (A,B) and COX-2 (C,D) in liver tissue 4 hours after the administration of saline or LPS. Immunoreactive COX-1 was seen in the sinusoidal lining cells in both saline- (A) and LPS-treated mice (B). On the other hand, the immunoreactivity with COX-2 was negative in saline-treated animals (C), whereas it was enhanced in the sinusoids after LPS treatment (D). One representative experiment of 2 animals were presented. Bar indicates 50 μm.

TXA_2 inhibition. However, others[33] have reported that ICAM-1 is involved in accumulation of leukocytes in the hepatic venules, but not in the sinusoids. Furthermore, the present study showed that OKY-046 did not significantly change the LPS-induced increase in the expression of PECAM-1, suggesting that microcirculatory dysfunction improved by TXA_2 inhibition is independent of PECAM-1 expression, and this is consistent with the findings of others.[33]

LPS administration to the isolated perfused liver resulted in a rapid and significant release of TXB_2 into the perfusate, suggesting that the liver is an important source of TXA_2, and that TXA_2 seems to be an inflammatory mediator in the early phase of endotoxemia. We measured the levels of TXB_2 in the effluent perfusate because the levels of TXs and PGs were artificially elevated with ease by mechanical stimulation.[20] In the liver, in response to LPS, TXA_2 is released from nonparenchymal cells (*i.e.*, Kupffer cells[6] and sinusoidal endothelial cells).[34] Of these, Kupffer cells are a major source of TXA_2. However, the possibility that activated platelets are productive sources of TXA_2 *in vivo* cannot be excluded.

To explore whether COX-1 and COX-2 activities are involved in hepatic microcirculatory dysfunction during endotoxemia, mice were treated with the selective COX-1 inhibitor SC-560 and the selective COX-2 inhibitor NS-398. Both SC-560 and NS-398 significantly reduced liver injury and hepatic microcirculatory dysfunction in response to LPS. These results suggest that COX-1 and COX-2 are involved in liver injury. In fact, the levels of ALT activity after LPS combination with galactosamine were significantly decreased in COX-2-deficient mice.[12] A selective COX-2 inhibitor, FK3311, limited liver injury in dogs caused by ischemia/reperfusion and restored he-

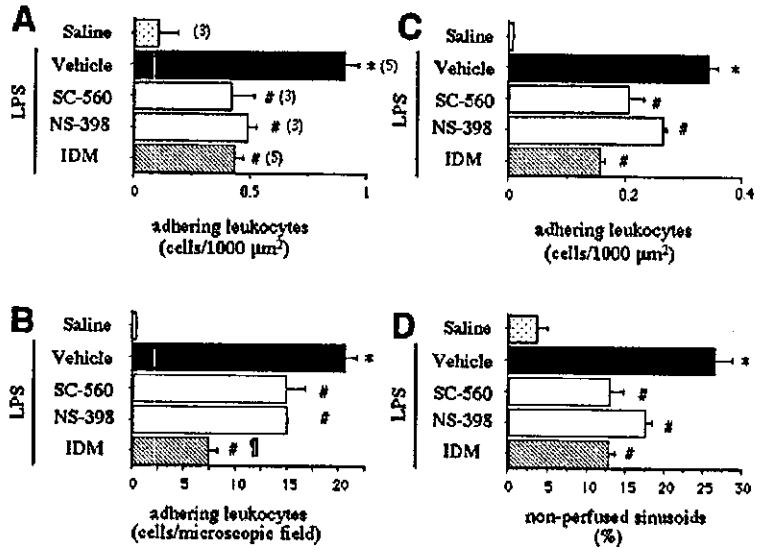

Fig. 10. Effects of SC-560 (10 mg/kg, p.o.), NS-398 (10 mg/kg, s.c.), and indomethacin (IDM) on (A) the numbers of leukocytes adhering to the portal venules, (B) the numbers of leukocytes adhering to the sinusoids, (C) the numbers of leukocytes adhering to the central venules, and (D) the percentage of non-perfused sinusoids after LPS administration. The numbers of adhering leukocytes and of sinusoids were determined 4 hours after LPS injection. Numbers in parentheses indicate number of animals. Data are shown as means ± SEM. *$P < .05$ versus Saline-treated mice; #$P < .05$ versus LPS-treated mice; ¶$P < .05$ versus NS-398-treated mice and SC-560-treated mice.

patic tissue blood flow.[13] Inhibition of COX-2 with NS-398 improved survival from sepsis induced by cecal ligation and puncture in mice.[35] In contrast, Leach et al.[36] reported that inhibition of COX-2 with NS-398 failed to attenuate liver injury elicited by LPS in rats. The reasons for these discrepancies remain unclear, though they may be caused by differences in the animals and the doses of drugs used.

The contribution of PGs generated through the action of COX-1 to hepatic microcirculatory dysfunction and leukocyte adhesion can be estimated from the reduction in the leukocyte adhesion variables after the administration of a COX-1 selective inhibitor, SC-560. This agent used in the present experimental conditions exhibits good selectivity to COX-1. The same was also true in the case of COX-2 inhibition using the COX-2 inhibitor NS-398. In the portal venules, the adhesion of leukocytes were reduced equally by SC-560 and NS-398. This indicates that the PGs generated through COX-1 and COX-2 enhanced the adhesion equally. But, indomethacin did not inhibit the adhesion more intensely than SC-560 and NS-398 in portal venules in the present experiment, although this inhibitor blocks both COX-1 and COX-2. We supposed that there might be a threshold concentration of TXA_2 generated in the microvasculature to induce leukocyte adhesion. Without treatment with COX inhibitors, the amount of TXA_2 generated may be more than the threshold concentration of TXA_2 when either COX-1 or COX-2 is inhibited. If PGs are generated through the action of COX-1 and COX-2, and if no alternative pathway for PG generation is present, the inhibition of either COX-1 or COX-2, or both, certainly reduces the PG levels, which may be lower than the threshold concentration. If the inhibition of either COX-1 or COX-2 is enough to lower the TXA_2 levels below the threshold concentration, the effects of indomethacin are not different from those observed under the inhibition of COX-1 or COX-2. Judging from the results of the perfusion experiment, sites of TXA_2 generation were certainly present in the liver. So, the concentration of TXA_2 may be higher in the sinusoids or in the central venules than in the portal venules. TXA_2 at a concentration over the threshold concentration may induce adhesion in a concentration-dependent manner. In fact, we can observe the effects of indomethacin to be the sum of the inhibition of COX-1 and that of COX-2 in the sinusoids or central venules, where the TXA_2 concentration may be higher than that in portal venules.

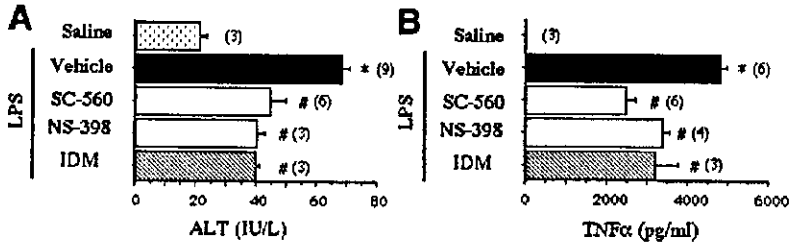

Fig. 11. Effects of SC-560 (10 mg/kg, p.o.), NS-398 (10 mg/kg, s.c.), and indomethacin (IDM 10 mg/kg, p.o.) on (A) serum ALT activity and (B) the serum concentrations of TNFα after LPS administration. Numbers in parentheses indicate number of animals. Data are shown as means ± SEM. *$P < .05$ versus Saline-treated mice; #$P < .05$ versus LPS-treated mice.

In conclusion, our present study clarifies the important role played by TXA_2 in hepatic microcirculatory dysfunction elicited by LPS administration, although factors other than TXA_2 were reported previously.[37–42] LPS-induced hepatic microcirculatory dysfunction was associated with TXA_2 generation in the liver. The inhibitory effects of TXA_2 synthase inhibitor and TXA_2 receptor antagonist on the hepatic response to LPS were similar to the effects of selective COX-1 and COX-2 inhibitors, suggesting that endogenous TXA_2 derived from both COX-1 and COX-2 participate in LPS-induced liver injury by enhancement of TNFα production. TP receptor signaling may be related to the upregulation of expression of an adhesion molecule, ICAM-1.

Acknowledgment: The authors thank Michiko Ogino and Osamu Katsumata for their technical assistance. The authors also express their thanks to C.W.P. Reynolds for correcting the English of this manuscript.

References

1. McCuskey RS. Hepatic microvascular response to endotoxemia and sepsis. In: Messmer K, Menger MD, eds. Progress in Applied Microcirculation. Basel: Karger, 1993;19:76–84.
2. Vollmar B, Rüttinger D, Wanner GA, Leiderer R, Menger MD. Modulation of Kupffer cell activity by gadolinium chloride in endotoxemic rats. Shock 1996;6:434–441.
3. Chensue SW, Terebuh PD, Remick DG, Scales WE, Kunkel SL. In vivo biologic and immunohistochemical analysis of interleukin-1 alpha, beta and tumor necrosis factor during experimental endotoxemia. Kinetics, Kupffer cell expression, and glucocorticoid effects. Am J Pathol 1991;138: 395–402.
4. Luster MI, Germolec DR, Yoshida T, Kayama F, Thompson M. Endotoxin-induced cytokine gene expression and excretion in the liver. HEPATOLOGY 1994;19:480–488.
5. Matsumoto Y, Ito Y, Hayashi I, Majima M, Ishii K, Katagiri H, Kakita A. Effect of FR167653, a novel inhibitor of tumor necrosis factor alpha and interleukin-1 beta synthesis on lipopolysaccharide-induced hepatic microvascular dysfunction in mice. Shock 2002;17:411–415.
6. Decker K. Biologically active products of stimulated liver macrophages. Eur J Biochem 1990;192:245–361.
7. Altavilla D Squadrito F, Canale P, Ioculano M, Squadrito G, Campo GM, Serrano M, et al. G619, a dual thromboxane synthase inhibitor and thromboxane A_2 receptor antagonist, inhibits tumor necrosis factor-α biosynthesis. Eur J Pharmacol 1995;286:31–39.
8. Ishiguro S, Arii S, Monden K, Adachi Y, Funaki N, Higashitsuji H, Fujita S, et al. Identification of the thromboxane A_2 receptor in hepatic sinusoidal endothelial cells and its role in endotoxin-induced liver injury in rats. HEPATOLOGY 1994;20:1281–1286.
9. Karck U, Peters T, Decker K. The release of tumor necrosis factor from endotoxin-stimulated rat Kupffer cells is regulated by prostaglandin E_2 and dexamethasone. J Hepatol 1988;7:352–361.
10. Otto JC, Smith WL. Prostaglandin endoperoxide synthases-1 and -2. J Lipid Mediat Cell Signal 1995;12:139–156.
11. Ruetten H, Thiemermann C. Effect of calpain inhibitor I, an inhibitor of the proteolysis of IκB, on the circulatory failure and multiple organ dysfunction caused by endotoxin in the rat. Br J Pharmacol 1997;121:695–704.
12. Dinchuk JR, Car BD, Focht RJ, Johnson JJ, Jaffee BD, Covington MB, Contel NR, et al. Renal abnormalities and an altered inflammatory response in mice lacking cyclooxygenase II. Nature 1995;378:406–409.
13. Sunose Y, Takeyoshi I, Ohwada S, Tsutsumi H, Iwazaki S, Kawata K, Kawashima Y, et al. The effect of cyclooxygenase-2 inhibitor FK3311 on ischemia-reperfusion injury in a canine total hepatic vascular exclusion model. J Am Coll Surg 2001;192:54–62.
14. Hanasaki K, Nagasaki T, Arita H. Characterization of platelet thromboxane A_2/prostaglandin H_2 receptor by a novel thromboxane receptor antagonist, [3H]S-145. Biochem Pharmacol 1989;38:2007–2017.
15. Smith CJ, Zhang Y, Koboldt CM, Muhammad J, Zweifel BS, Shaffer A, Talley JJ, et al. Pharmacological analysis of cyclooxygenase-1 in inflammation. Proc Natl Acad Sci U S A 1998;95:13313–13318.
16. Futaki N, Yoshikawa K, Hamasuka Y, Arai I, Higuchi S, Iizuka H, Otomo S. NS-398, a novel non-steroidal anti-inflammatory drug with potent analgesic and antipyretic effects, which causes minimal stomach lesions. Gen Pharmacol 1993;24:105–110.
17. Xiao CY, Hara A, Yuhki K, Fujino T, Ma H, Okada Y, Takahata O, et al. Roles of prostaglandin I2 and thromboxane A2 in cardiac ischemia-reperfusion injury. Circulation 2001;104:2210–2205.
18. Post S, Palma P, Rentsch M, Gonzalez MD, Menger MD. Hepatic reperfusion injury following cold ischemia in the rat: potentials and quantitative analysis by in vivo fluorescence microscopy. In: Messmer K, Menger MD, eds. Progress in Applied Microcirculation. Basel: Karger, 1993;19:152–166.
19. Suematsu M, Goda N, Sano T, Kashiwagi S, Shinoda Y, Ishimura Y. Carbon monoxide: an endogenous modulator of sinusoidal tone in the perfused rat liver. J Clin Invest 1995;96:2431–2437.
20. Suzuki Y, Ueno A, Kawamura M, Nishiyama K, Katori M, Okabe H. Prostaglandin levels in the rat resting gastric wall and enhancement of prostaglandin E_2 generation after administration of mild hyperosmotic saline solution into the gastric lumen. Eicosanoids 1990;3:23–27.
21. Boku K, Ohno T, Saeki T, Hayashi H, Hayashi I, Katori M, Murata T, et al. Adaptive cytoprotection mediated by prostaglandin I_2 is attributable to sensitization of CGRP-containing sensory nerves. Gastroenterology 2001; 120:134–143.
22. Majima M, Isono M, Ikeda Y, Hayashi I, Hatanaka K, Harada Y, Katsumata O, et al. Significant roles of inducible cyclooxygenase (COX)-2 in angiogenesis in rat sponge implants. Jpn J Pharmacol 1997;75:105–114.
23. Molle WV, Berghe JV, Brouchaert P, Libert C. Tumor necrosis factor-α-induced lethal hepatitis: pharmacological intervention with verapamil, tannic acid, picotamide and K76COOH. FEBS Lett 2000;467:201–205.
24. Shirabe K, Kin S, Shinagawa Y, Chen S, Payne WD, Sugimachi K. Inhibition of thromboxane A_2 activity during warm ischemia of the liver. J Surg Res 1996;61:103–107.
25. Sugawara Y, Harihara Y, Takayama T, Makuuchi M. Suppression of cytokine production by thromboxane A_2 inhibitor in liver ischemia. Hepatogastroenterology 1998;45:1781–1786.
26. Nagai H, Shimazawa T, Yakuo I, Aoki M, Kosa A, Kasahara M. The role of thromboxane A_2 (TXA_2) in liver injury in mice. Prostaglandins 1989; 38:439–446.
27. Kuhn DC, Stauffer JL, Gaydos LJ, Lacey SL, Demers LM. An inhibitor of thromboxane production attenuates tumor necrosis factor release by activated human alveolar macrophages. Prostaglandins 1993;46:195–205.
28. Grandel U, Fink L, Blum A, Heep M, Buerke M, Kraemer H-J, Mayer K, et al. Endotoxin-induced myocardial tumor necrosis factor-α synthesis depresses contractility of isolated rat hearts. Evidence for a role of sphingosine and cyclooxygenase-2-derived thromboxane production. Circulation 2000;102:2758–2764.
29. Ishizuka T, Kawakami M, Hidaka T, Matsuki Y, Takamizawa M, Suzuki K, Kurita A, et al. Stimulation with thromboxane A_2 (TXA_2) receptor agonist enhances ICAM-1, VCAM-1 or ELAM-1 expression by human vascular endothelial cells. Clin Exp Immunol 1998;112:464–470.
30. Sakamoto S, Okanoue T, Itoh Y, Nakagawa Y, Nakamura H, Morita A, Daimon Y, et al. Involvement of Kupffer cells in the interaction between neutrophils and sinusoidal endothelial cells in rats. Shock 2002;18:152–157.
31. Neubauer K, Ritzel A, Saile B, Ramadori G. Decrease of platelet-endothelial cell adhesion molecule 1-gene-expression in inflammatory cells and in endothelial cells in the rat liver following CCl(4)-administration and in vitro after treatment with TNFalpha. Immunol Lett 2000;74:153–164.

32. Essani NA, Fisher MA, Farhood A, Manning AM, Smith CW, Jaeschke H. Cytokine-induced upregulation of hepatic intercellular adhesion molecule-1 messenger RNA expression and its role in the pathophysiology of murine endotoxin shock and acute liver failure. HEPATOLOGY 1995;21:1632–1639.
33. Chosay JG, Fisher MA, Farhood A, Ready KA, Dunn CJ, Jaeschke H. Role of PECAM-1 (CD31) in neutrophil transmigration in murine models of liver and peritoneal inflammation. Am J Physiol 1998;274: G776–G782.
34. Rieder H, Ramadori G, Allmann K-H, Meyer K-H, Büschenfelde M. Prostanoid release of cultured liver sinusoidal endothelial cells in response to endotoxin and tumor necrosis factor. J Hepatol 1990;11:359–366.
35. Mack Strong VE, Mackrell PJ, Concannon EM, Mestre JR, Smyth GP, Schaefer PA, Stapleton PP, et al. NS-398 treatment after trauma modifies NF-κB activation and improves survival. J Surg Res 2001;98,40–46.
36. Leach M, Hamilton LC, Olbrich A, Wray GM, Thiemermann C. Effects of inhibitors of the activity of cyclo-oxygenase-2 on the hypotension and multiple organ dysfunction caused by endotoxin: a comparison with dexamethasone. Br J Pharmacol 1998;124:586–592.
37. Doi F, Goya T, Torisu M. Potential role of hepatic macrophages in neutrophil-mediated liver injury in rats with sepsis. HEPATOLOGY 1993;17:1086–1094.
38. Shiratori Y, Tanaka M, Hai K, Kawase T, Shirna S, Sugimoto T. Role of endotoxin-responsive macrophages in hepatic injury. HEPATOLOGY 1990; 11:183–192.
39. Dahm LJ, Schultze AE, Roth RA. Activated neutrophils injure the isolated, perfused rat liver by an oxygen radical-dependent mechanism. Am J Pathol 1991;139:1009–1020.
40. Kurose I, Kato S, Ishii H, Fukumura D, Miura S, Suematsu M, Tsuchiya M. Nitric oxide mediates lipopolysaccharide-induced alteration of mitochondrial function in cultured hepatocytes and isolated perfused liver. HEPATOLOGY 1993;18:380–388.
41. Sakaguchi T, Nakamura S, Suzuki S, Oda T, Ichiyama A, Baba S, Okamoto T. Participation of platelet-activating factor in the lipopolysaccharide-induced liver injury in partially hepatectomized rats. HEPATOLOGY 1999;30:959–967.
42. Feder LS, Todaro JA, Laskin DL. Characterization of interleukin-1 and interleukin-6 production by hepatic endothelial cells and macrophages. J Leukocyte Biol 1993;53:126–132.

ELSEVIER

International Journal of Cardiology 98 (2005) 245–252

International Journal of Cardiology

www.elsevier.com/locate/ijcard

Activated leukocytes and endothelial cells enhance retention of ultrasound contrast microspheres containing perfluoropropane in inflamed venules

Takanori Yasu[a,*], Yigal Greener[b], Edward Jablonski[b], Anne L. Killam[b], Shunichi Fukuda[a], Makoto Suematsu[c], Shinichiro J. Tojo[d], Geert W. Schmid-Schönbein[a]

[a] *Department of Bioengineering, University of California San Diego, La Jolla, CA 92093-0412, USA*
[b] *Molecular Biosystems Inc., San Diego, CA 92121-2789, USA*
[c] *Department of Biochemistry, Keio University, Tokyo, Japan*
[d] *Sumitomo Pharmaceutical Co. Ltd., Osaka, Japan*

Received 28 May 2003; accepted 12 October 2003
Available online 12 April 2004

Abstract

Purpose: To characterize the flow dynamics of albumin ultrasound contrast microspheres containing perfluoropropane (PFP) in normal and inflamed microvasculature. *Materials and methods:* Mesenteric microvessels of rats were examined after an intravenous injection of fluorocein-labeled erythrocytes or PFP microspheres by fluorescence intravital microscopy with and without local application of 10^{-8} M platelet activating factor (PAF) as an experimental form of inflammation. *Results:* All the microspheres passed freely through arterioles and capillaries. Mean velocities of the microspheres in each vessel were closely correlated with those of erythrocytes. Only a minor fraction of the microspheres was retained in the venules (≥ 0.1 s stoppage) by attachment to endothelial cells. The frequency of microsphere retention in venules was significantly enhanced by PAF ($2.6 \pm 2.1\%$, $P < 0.01$ vs. control), especially in regions with leukocyte adhesion. Treatment with a monoclonal antibody to intercellular adhesion molecule-1, P-selectin or the common leukocyte antigen inhibited PAF-induced microsphere retention in venules ($P < 0.05$). In the inflamed microcirculation, a small subgroup of microspheres becomes attached to venular endothelial cells in regions with leukocyte adhesion via interaction among microspheres, activated leukocytes and endothelial cells via adhesion molecules. *Conclusion:* In inflamed microcirculation, a small subgroup of microspheres becomes attached to venular endothelial cells in regions with leukocyte adhesion via interaction among microspheres, activated leukocytes and endothelial cells via adhesion molecules. These results suggest that ultrasonography with microspheres has the potential to evaluate inflammatory site distribution as well as tissue perfusion.

Keywords: Contrast; Echocardiography; Leukocyte; Membrane adhesion; Microcirculation

1. Introduction

The development of ultrasound contrast microspheres has opened a novel direction for study of myocardial microcirculation in a clinical setting [1,2]. But as a basis for the clinical observations, the rheological behavior of microspheres in vivo needs to be further examined under different conditions [2,3]. Albumin microspheres persist in the inflamed microcirculation for a longer period than erythrocytes after ischemia–reperfusion [4,5]. A recent report has suggested that activated leukocytes attach and phagocytose microspheres in vitro and in vivo [6]. Tissues subjected to inflammation such as ischemia–reperfusion are associated with microvascular alterations including increases in leukocyte adherence and extravasation in post-capillary venules, increased vascular permeability, endothelial cell dysfunction, capillary plugging, and hemorrhage [7–11]. Local application of platelet activating factor (PAF) induces microvascular inflammation in the mesenteric microcirculation [7,12]. Hence, the aims of this study were to examine the behavior of ultrasound contrast microspheres with an albumin shell and containing perfluoropropane (PFP) in the normal and experimentally inflamed microcirculation by local application of PAF. We focused on

* Corresponding author. Present address: Cardiovascular Division, Department of Integrated Medicine I, Omiya Medical Center, Jichi Medical School, Omiya, Saitama 330-8503, Japan. Tel.: +81-48-647-2111; fax: +81-48-648-5188.
E-mail address: tyasu@omiya.jichi.ac.jp (T. Yasu).

0167-5273/$ - see front matter © 2004 Elsevier Ireland Ltd. All rights reserved.
doi:10.1016/j.ijcard.2003.10.042

interaction among PFP microspheres, leukocytes and endothelial cells in the microcirculation.

2. Materials and methods

2.1. Preparation of fluorescein-labeled PFP microspheres

Human albumin 5% solution 250 ml was adjusted to pH 8.5 with 1 M NaOH under vigorous stirring. A 10-fold molar excess of fluorescein isothiocyanate (FITC), isomer I (0.75 g) was dissolved in 5 ml *N,N*-dimethylformamide and added dropwise to the albumin solution under continuous stirring at room temperature. The pH was readjusted back to a value of 8.5 after the addition of each ml of FITC. The clear orange reaction mixture was immediately filtered under sterile conditions and incubated for 10 h at 4 °C. Free fluorescein was removed by exhaustive dialysis against 4 × 4 l PBS, pH 6.9. The dialyzed conjugate was again filtered. The estimated conjugation ratio was 2: 3 (FITC: albumin). The FITC-albumin solution was diluted to 1% protein with normal saline and the microspheres were prepared using the 2-in. Gaulin colloid mill model 2F (APV Gaulin, Wilmington, MA) operating at 70 °C.

Microsphere preparations chilled to 18 °C were gently washed and resuspended to remove any remaining FITC-labeled albumin that was not part of the microspheres. The products were collected separately into 5-l plastic bags and stored at 4 °C. The in vitro diameter of 1000 FITC-labeled PFP microspheres was 4.0 ± 2.2 μm (mean ± S.D.) (n = 1000), 3.8 μm (median), 2.0 μm (10 percentile), 6.2 μm (90 percentile). The PFP microsphere concentration was approximately 8.2×10^8/ml. This dose of microspheres is about 2-fold higher than that used clinically with no adverse side effects.

2.2. PKH-labeled erythrocyte preparation

Erythrocytes from separate donor rats were labeled with PKH-26 (Zynaxis Cell Science, Malvern, PA) according to the manufacturer's instructions. PKH-labeled erythrocytes are stable in vivo [3,13,14]. This enhanced stability allowed us to determine the erythrocyte velocity in vivo throughout the experiment after a single bolus injection.

2.3. Animal preparation

All animal procedures were reviewed and approved by the University of California, San Diego, Animal Subjects Committee. Fifty male Wistar rats (13–15 weeks of age, 280–380 g; Charles River Breeding Laboratories, Wilmington, MA) were used for this study. After general anesthesia (pentobarbital sodium, 40 mg/kg i.m.) a catheter (PE-50 tubing, Clay Adams) was inserted into the left femoral artery and systemic blood pressure was continuously monitored. Another catheter was inserted into the left femoral vein for injections. The animals were placed on a water heating pad maintained at 37 °C. For the mesentery preparation, the abdomen was opened by a small midline incision and the ileocecal part of the mesentery was carefully exteriorized and draped over a thin plastic sheet to minimize the exposure to air during intravital microscopy. The preparation was maintained at 37 °C and continuously superfused (1.0 ml/min) with Krebs–Henseleit bicarbonate-buffered solution saturated with a 95% N_2 and 5% CO_2 gas mixture to maintain physiological pH.

2.4. Intravital fluorescence microscopy

The mesenteric microcirculation was observed through an intravital fluorescence microscope (× 25, water-immersion objective lens, Leitz, Wetzlar, Germany) using a silicone intensified target camera (Series 66, Dage-MTI, Michigan City, IN). To elicit fluorescent images, the preparation was illuminated with a 200-W mercury lamp. The light was passed through a quartz collector, heat filter, and a 420- to 490-nm or a 515- to 560-nm excitation filter (Leitz) to epi-illuminate the preparation for observation of FITC-labeled microspheres (emission wavelength, 520 nm) or PKH 26-labeled erythrocytes (emission wavelength 580 nm). All fluorescent micrographs were recorded with a fixed gain control setting on the silicone intensified target tube camera. Bright field illumination was provided by a 250-W halogen light source with heat filter. The video vertical frame rate of the camera was 30/s. The overall magnification on the TV monitor was approximately × 910. The images were stored on VHS tapes, using a videocassette recorder (Model AG-6300, Panasonic, Tokyo, Japan) for off-line analysis.

All images were compiled and analyzed on a Macintosh computer with public domain National Institute of Health image software (Version 1.60). The computer was calibrated in the x–y planes using a calibration reticule (10-μm divisions). The vessel diameters refer to inner lumen measurements; no corrections were made for non-circular cross-sections [15]. The velocity of labeled microspheres and erythrocytes in arterioles, capillaries and venules was measured twice based on frame by frame analysis [3], and each pair of measurements were averaged.

We defined retention of microspheres as stoppage in vessels persisting for 0.1 sec (three frames) or longer because no erythrocytes were retained for such a period during constant shear rates [3]. Adhesive leukocytes were defined when they remained stationary on the EC for at least a period of 30 s during constant shear rates [3]. When a microsphere became stationary in microvessels for more than 2 s, we observed the field under bright field illumination for a few seconds to determine whether its stoppage was due to vascular obstruction and also whether the stationary microsphere had attached to a leukocyte

or endothelium. The frequency of microsphere retention in vessels by attachment with the endothelial cells was calculated by dividing the number of retained microspheres per 200 μm length of each vessel by the total number of microspheres observed in that vessel [3]. In selected experiments, a 40× objective lens (Leitz) was used to visualize retained microspheres in venules in more detail.

2.5. In vivo protocol

2.5.1. Kinetics of labeled microspheres in normal microcirculation

The intravital microscopy of rat mesentery was conducted by focusing on the median plane of the microvessel except when it was necessary to focus on retained microspheres. After exposing the mesentery, steady superfusion was maintained for 15 min. Injection of 0.1 ml PKH-labeled erythrocytes was carried out via the left femoral vein. After recording fluorescent images for PKH-labeled erythrocytes in selected arterioles, capillaries, and venules, 0.1–0.2 ml/kg of FITC-labeled PFP microspheres was injected over a 5-s period via the femoral vein. The catheter was flushed with 0.25 ml saline after each injection. Only one injection of PFP microspheres was given to each rat. Fourteen randomly selected arterioles with diameters ranging from 9 to 30 μm, 12 capillaries with diameters ranging from 5 to 7 μm, and 26 venules with diameters ranging from 10 to 50 μm in 16 rats were examined for PFP microspheres. After microsphere injection (approximately 70 min after the injection), 10 fields of venules in each rat were randomly recorded to determine whether any of the microspheres had migrated into the extravascular space under non-inflammatory control conditions.

2.5.2. Kinetics of labeled microspheres in inflamed microcirculation

To observe the behavior of labeled PFP microspheres in the inflamed microvessels, 10^{-8} M PAF (Sigma St. Louis, MO) was added to the superfusion for 30 min following a period of 10 min with steady superfusion. In this protocol, the injection and observation procedures were as described above. Six randomly selected arterioles ranging in diameter from 9 to 30 μm, 7 capillaries with diameters of 5 to 7 μm, and 22 venules with diameters ranging from 10 to 50 μm in 16 rats were examined. Seventy min after the microsphere injection, 10 fields of venules in each rat were recorded to determine whether or not microspheres had migrated into the extravascular space after PAF application.

Eighteen rats were treated with several kinds of anti-rat monoclonal antibodies (MoAbs) to inhibit each function. An anti-rat leukocyte MoAb directed against a rat leukocyte common antigen, CD45 (MRC OX-1, Serotec, London,

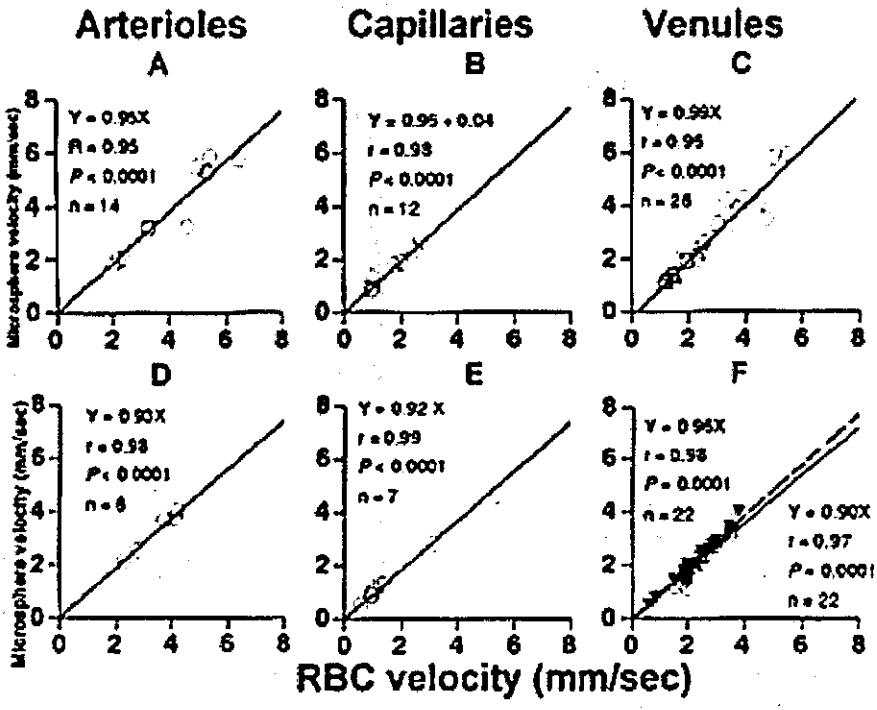

Fig. 1. Correlation between mean velocities of red blood cells (RBC) and those of perfluoropropane (PFP)-containing albumin microspheres in individual arterioles, capillaries, and venules under control conditions (panels A, B, and C) and after local application of 10^{-8} M platelet activating factor (PAF) for 30 min (panel D, E, and F). After omitting the data of retained PFP microspheres in panel F (closed triangles), the mean velocities of the microspheres show more identical ($Y=0.96X$, $R=0.98$, $P=0.0001$) with that of RBC rather than the microspheres including retained ones. Data were obtained from 16 rats.

England) (30 μg/kg) [16,17] was administered to four rats intravenously 1 h before laparotomy to assess the interaction among microspheres, leukocytes and endothelial cells in the leukopenic model Leukocyte counts were taken before and 40 min after antibody administration. An anti-rat MoAb to intercellular adhesion molecule-1 (ICAM-1) (1A29, Seikagaku Tokyo, Japan) (1.0 mg/kg, $n=5$) [17] or P-selectin (ARP2.4, Sumitomo Pharmaceutical, Tokyo, Japan) (1.0 mg/kg, $n=5$) [18,19] was administered intravenously to 10 rats 1 h before laparotomy to explore the function of adhesion molecules on the endothelial cells during the process of microsphere retention in inflamed postcapillary venules. Sodium azide was dialyzed from all the MoAbs before use. PAF (10^{-8} M) was added to the superfusion for 30 min after 15 min of steady superfusion. PFP microspheres (0.1–0.2 ml/kg) were injected into the femoral vein as described above. Randomly selected 21–30 venules ranging in diameter from 10 to 50 μm were observed for each antibody treatment.

2.5.3. Statistics

All results are expressed as means ± S.D. Correlation between the mean velocity of the labeled microspheres and that of the labeled erythrocytes in individual vessels was assessed by Pearson's correlation coefficient. To quantify the association of adhering leukocyte number and frequency of microsphere retention in venules, Pearson's correlation coefficient was calculated. The frequency of microsphere retention and the adherent leukocyte number in venules were compared among controls, local PAF application without any MoAbs, local PAF application with each MoAb against CD45, ICAM-1, or P-selectin by ANOVA and a Scheffe-type multiple comparison test. Probability levels below 0.05 were considered statistically significant. The statistical analysis was carried

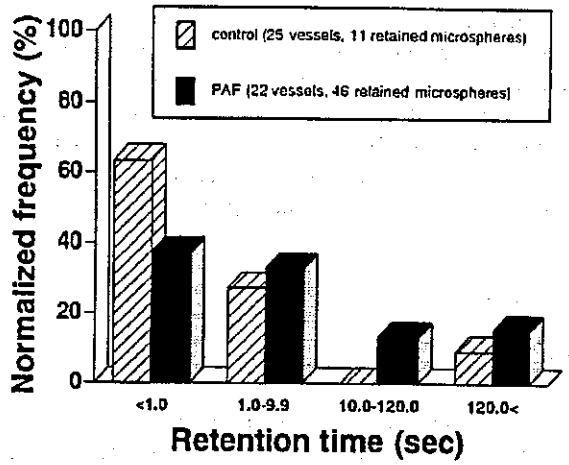

Fig. 3. Normalized frequency (%) of perfluoropropane-containing microsphere retention time in venules with diameters between 10 and 50 μm under control conditions and after local application of 10^{-8} M platelet activating factor.

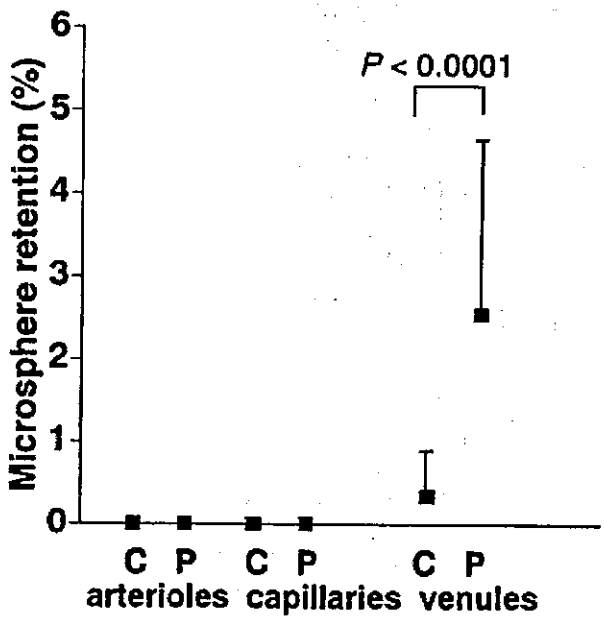

Fig. 2. Frequency of perfluoropropane-containing albumin microsphere retention (≥ 0.1 s stoppage) in microvessels under control conditions and after local application of 10^{-8} M platelet activating factor (PAF). Under control condition and local 10^{-8} M PAF application, all microspheres passed through arterioles and capillaries without retention. The frequency of microsphere retention in the venules significantly increased after PAF application (2.6 ± 2.1%) compared with the control (0.3 ± 0.6%).

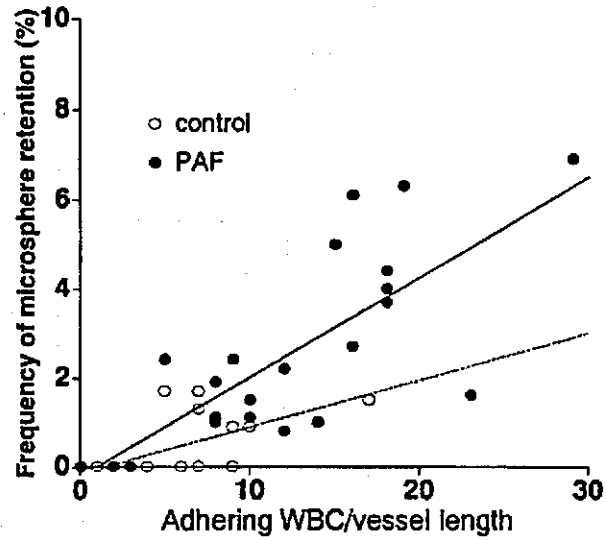

Fig. 4. PFP-containing albumin microsphere retention frequency compared with white blood cell (WBC) adherence in 200-μm-long venules. Data were obtained from five rats as controls and four rats after PAF application. Retention frequency of microsphere and WBC adherence roughly correlated in venules under both control conditions ($Y=0.11X-0.17$, $r=0.67$, $P=0.0001$, $n=26$) and after applying 10^{-8} M platelet activating factor (PAF) ($Y=0.23X-0.24$, $r=0.76$, $P<0.0001$, $n=22$).

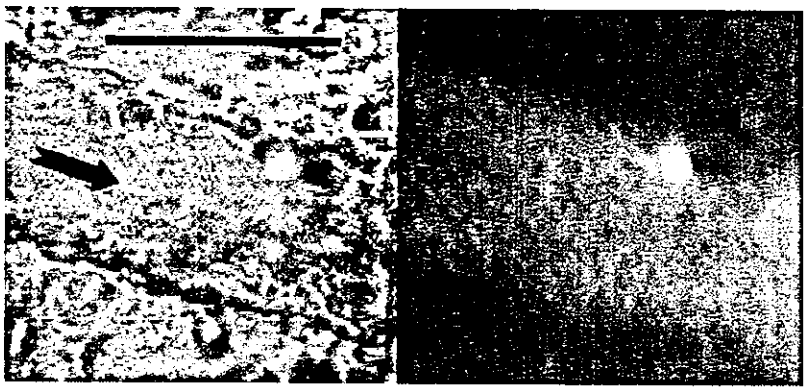

Fig. 5. Micrographs showing a retained FITC-labeled perfluoropropane (PFP)-containing albumin microsphere attached to endothelium and adhering leukocytes in a venule after local application of 10^{-8} M platelet activating factor. One venule with a diameter of 36 μm is imaged under transillumination and epi-illumination at 480 nm in the left panel, and under epi-illumination in the right panel. The flow of the venule is from left to right. An FITC-labeled microsphere is retained adjacent to adhering leukocytes 3 min after microsphere injection.

out using Stat View IV software (Abacus Concepts, Berkeley, CA).

3. Results

Systemic blood pressure and heart rate did not significantly change during the three min observation period after injection of FITC-labeled PFP microspheres (data not shown). Under control conditions, all PFP microspheres passed rapidly along arterioles and capillaries without being impeded. Mean velocities of FITC-labeled PFP microspheres in individual mesenteric microvessels were correlated with those of PKH-labeled erythrocytes in arterioles, capillaries, and venules even after the application of PAF (Fig. 1a,b,c). A few PFP microspheres (11 of 1993) were transiently (0.1–131 s) retained on the endothelial cells of venules but not in arterioles or capillaries (Fig. 2). There was no extravascular migration of PFP microspheres in the 60 observation fields under control conditions 10 min after injection of microspheres.

Local PAF 10^{-8} M application induced adherence and extravasation of leukocytes in postcapillary venules but not in arterioles or capillaries (Fig. 2). The frequency of PFP microsphere retention in the venules was slightly but significantly increased after the local application of PAF (Fig. 2, $P<0.01$ vs. control). The mean velocities of the microspheres except retained ones in individual venules were identical with the mean velocities of erythrocytes (Fig. 1). The retention time of individual PFP microspheres in venules tended to increase after PAF application (Fig. 3). PFP microsphere retention occurred predominantly at sites of enhanced leukocyte adhesion (Figs. 4 and 5). Thirty out of thirty-three (91%) microspheres retained in venules after PAF application were attached to (or phagocytosed by) leukocytes adhering to the endothelial cells (Fig. 5). Three out of the above thirty microspheres were attached only to adhering leukocytes not to the endothelial cells (Table 1). All of the rolling microspheres imaged both under bright field or fluorescence illumination ($n=12$) attached to rolling leukocytes on the venular endothelial cells.

After administration of the antibody against CD45, the systemic white blood cell count was significantly reduced from 6750 ± 501 to 5050 ± 340 cells/mm^3 ($n=4$, $P<0.01$). The number of adhering leukocytes in venules after PAF application was significantly decreased by each MoAb treatment (MoAb to CD45, 6 ± 3 adhering leukocytes per 200 μm length of venules; MoAb to ICAM-1, 7 ± 2; MoAb to P-selectin, 3 ± 3, all $P<0.05$ vs. without MoAb treatment, 12 ± 7). The frequency of PFP-containing microsphere retention in venules was also significantly inhibited by the MoAbs to CD45 ($1.0 \pm 1.0\%$, $P<0.01$), ICAM-1 ($1.7 \pm 1.9\%$, $P<0.05$) and P-selectin ($0.6 \pm 1.5\%$, $P<0.01$) compared with that without MoAb treatment ($2.6 \pm 2.1\%$)

Table 1
The effect of monoclonal antibody against CD45, ICAM-1 and P-selectin on the spatial relationship between retained PFP-containing microspheres and adhering leukocytes in venules under local application of 10^{-8} M platelet activating factor

	Microspheres attached to adhering leukocytes	Microspheres not attached to adhering leukocytes	Total
Antibody (−)	30 (91%)	3 (9%)	33
CD45	8 (80%)	2 (20%)	10
ICAM-1	8 (80%)	2 (20%)	10
P-selectin	2 (67%)	1 (33%)	3
Total	47	9	56

The data obtained from sharply focused retained perfluoropropane (PFP)-containing microspheres in the mesenteric venules (each group, $n=21-30$ vessels) of Wistar rats (each group, $n=4-6$ rats) under PAF application with/without treatment of the antibody against CD45, ICAM-1, or P-selectin. The treatments of the monoclonal antibody dominantly reduced the number of retained microspheres attached to adhering leukocytes in venules. Out of the 33 retained microspheres without any antibody treatment, 3 were attached only to adhering leukocytes not to the endothelial cells.